Aalto University
School of Engineering
Civil Engineering Department

State-of-the-art of mathematical models for chemical degradation of concrete

PERCO2 project/WP3 – Mathematical models for estimating concrete ageing

Abobaker Ba Ragaa and Fahim Al-Neshawy

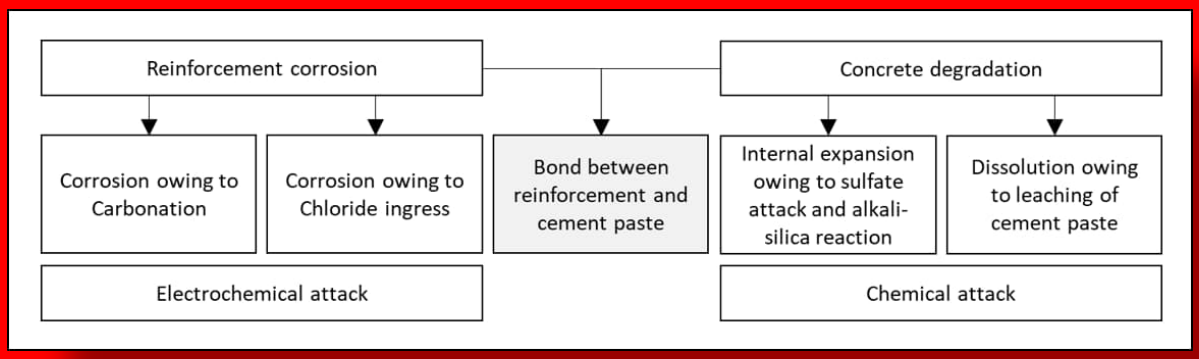

Aalto University School of Engineering, Department of Civil Engineering
PL 12100, FI-00076 AALTO
http://civileng.aalto.fi

Table of Contents

List of abbreviations

AAR	Alkali Aggregate Reaction
ACR	Alkali Carbonate Reaction
AI	Artificial Intelligence
ANN	Artificial Neural Network
ANS	Automated Neural Network Search
ASR	Alkali Silica Reaction
DEF	Delayed Ettringite Formation
FA	Fly Ash
GBFS	Granulated Blast Furnace Slag
ITZ	Interfacial Transition Zone
LILW	Low and Intermediate Level Waste
ML	Machine Learning
NPP	Nuclear Power Plant
OPC	Ordinary Portland Cement
PCC	Portland Cement Concrete
SCM	Supplementary Cementitious Materials
SEM	Scanning Electron Microscopy
SKB	Svensk Kärnbränslehantering AB
TDS	Total Dissolved Solids
TSA	Thaumasite Sulfate Attack

Cement Chemist Notations

Notation	Name
C_3S	Tricalcium Silicate (alite)
C_2S	Dicalcium Silicate (belite)
C_4AF	Tetracalcium Aluminoferrite
C_3A	Tricalcium Aluminate
AFm	Monosulfate aluminate phases
AFt	Trisulfate aluminate phases
$C-S-H$	Calcium Silicate Hydrate
CH	Calcium hydroxide (Portlandite)
$C_6A\bar{S}_3H_{32}$	Ettringite
$C_3S\bar{S}\bar{C}H_{15}$	Thaumasite
$C\bar{S}H_2$	Gypsum
$Ca(CO)_3$	Calcium carbonate (Calcite)
$C_4ACl_2H_{10}$	Friedel's salt
$M-S-H$	Magnesium Silicate Hydrate
$Mg(OH)_2$	Brucite

1. Introduction

1.1 Background and objectives of the Study

In Finland, nuclear energy is used widely, and therefore, ensuring safe long-term disposal of nuclear waste is of great importance. Radioactive waste should be stored safely, isolated from the environment, to avoid any hazards.

Reinforced concrete structures are used for various applications. The reliability of reinforced concrete makes it a preferred choice for many demanding cases. Concrete is tough, dense, and versatile. With a suitable mix, concrete structures can last for long durations, which adds to their mentioned qualities. However, with prolonged exposure to specific conditions, concrete can degrade over time. The study of the degradation pattern of reinforced concrete is therefore necessary to understand and assess the expected lifetime of the structure, especially in special structures, such as nuclear waste repositories.

In nuclear waste repositories, the contained nuclear waste is enclosed by multiple engineered barriers, to eliminate the associated risks. Concrete structures are used in the waste barriers, both as an enclosure for the waste, and potentially in the final backfilling of the tunnels. The concrete structure provides suitable qualities, being highly alkaline and dense, which is important for repository structures.

The use of concrete in waste repository can come with a few challenges, however, due to the demanding life-span requirements of the structure, which results in the exposure of concrete to degrading agents for elongated periods of time. This exposure, in the long run, can damage the reinforced concrete structure. Therefore, it is important to ensure that the barriers can sustain the exposure conditions sufficiently.

Due to the long exposure requirements in repository barriers, traditional testing approaches are not always very suitable. Therefore, the use of models and simulations, in addition to laboratory investigations of reinforced concrete is important when assessing the degradation properties of concrete in the nuclear waste repositories. Modelling results are not always very reliable, due to the complexity of concrete degradation, and the interconnected relationships of the reactive agents. In addition to that, simplifications are done in computational models, which can be critical in some cases. The use of isolated models specific to a certain case could also pose some reliability issues. Numerical models can also sometimes be used incorrectly. These challenges should be accounted for when a model is proposed.

The goal of this research is to focus on the degradation of reinforced concrete structures in repository conditions. Reinforced concrete is subjected to long exposure to degrading agents for a long duration, which affects its physical properties. The concrete degradation in the repositories can occur in both the operation phase, where the structure is surrounded by atmospheric environment, and post-closure phase where the tunnels are filled with groundwater, and the structure is in saturation. The concrete can be degraded via different mechanisms, such as chemicals that exist in the groundwater, the dissolution of cementitious materials from the concrete matrix, or the corrosion embedded steel reinforcement.

This research is also aimed at studying the use of modelling tools in reinforced concrete structures for long-term degradation. Modelling of concrete degradation is constantly evolving. The trend in current models is to consider more complex interactions, to develop a model that is accurate and reliable, which addresses the issues of some old models, that were quite simple, and inapplicable for most cases. Understanding kinetics of ionic interactions between cementitious materials and the exposure agents, and how those interactions progress with time is rather necessary, to further improve the conceptual model framework.

1.2 The Finnish LILW repositories

Nuclear waste in Finland arises from the two nuclear power plants at Olkiluoto and Loviisa, together comprising five reactor units. Other radioactive wastes, so called state-owned non-nuclear waste, arise from a number of facilities using radioisotopes in medical, research and industrial applications.

Teollisuuden Voima Oyj (TVO) takes care of its operational waste and power plant decommissioning waste. Their final disposal takes place in the operational waste repository (VLJ repository) at Olkiluoto. In Olkiluoto, the decommissioning waste generated during the dismantling of the plant units will also be deposited in facilities to be built in the same underground repository. The repository also accommodates radioactive waste generated in Finnish healthcare, industries, and research institutions. Waste is packed into concrete containers and transported to the repository using a radiation-protected vehicle. In the LILW repository, the concrete containers are placed into silos for low and intermediate level waste that have been excavated into the bedrock down to the level of 60–100 meters below the ground surface. Fortum Power and Heat Oy also takes care of its operational waste and power plant decommissioning waste and disposes them into an onsite repository in Loviisa at the depth of about 100 m. Figure 1 shows the location of the final disposal LILW waste repositories in Finland.

Low level waste consists of mixed waste contaminated by radioactive substances, which includes:

- Fire-protected fabrics
- Plastic wrappings and protective clothing used during maintenance work
- Replaced machinery parts and pipes from the nuclear power plant

The low level waste is packed into 200-liter drums and compressed to half of its volume using a hydraulic press. The radioactivity of the containers is measured before storage.

Intermediate level waste includes [1]:

- Ion-exchange resin from the circulating water cleaning system
- Liquids from various washing processes
- Sludge that forms when solid matter collects as sediment at the bottom of pumps and tanks.

Waste created in nuclear power plant operations is governed by either regular (non-radioactive) or radioactive waste management rules. Examples of regular waste include the waste created in a typical work environment, in goods transport, office tasks etc. Radioactive waste is classified as either low level, intermediate level (LILW) or high-level waste, based on how it was created, its original purpose and radioactivity level [2].

Figure 1. Locations of the final disposal sites for LILW waste in Finland and the existing nuclear sites.

LILW disposal facilities will have sufficient capacity for a long time to come. The need for the extension of LILW disposal facilities will become topical before the power plant units are decommissioned and dismantled.

1.3 Concrete structures in the LILW radioactive waste disposal

Finland currently has two nuclear waste repositories for LILW, one located at each nuclear power plant site. They are owned and operated by nuclear utilities for their own waste, with a small amount of space reserved for state-owned non-nuclear waste. Both repositories are excavated in the crystalline bedrock at the nuclear power plant site and are accessed via ramps (approximately 1 km long) for waste transport. A shaft with elevator access is provided for personnel only.

1.3.1 Reinforced concrete silo concept

The concept of silo type repositories has been implemented by TVO in the operational waste repository (VLJ repository) at Olkiluoto [3]. The scheme is illustrated in Figure 2. The silo concept consists of a case in which disposal containers and waste packages are placed on top of each other in several layers and the remaining space is planned to be filled with a backfill at the time of the closure. The experimental works [4]has been aimed at development of suitable concrete mixture composition, investigation of its properties in both fresh and hardened state, durability and resistance to groundwater, corrosion of reinforcement and degradation processes of concrete.

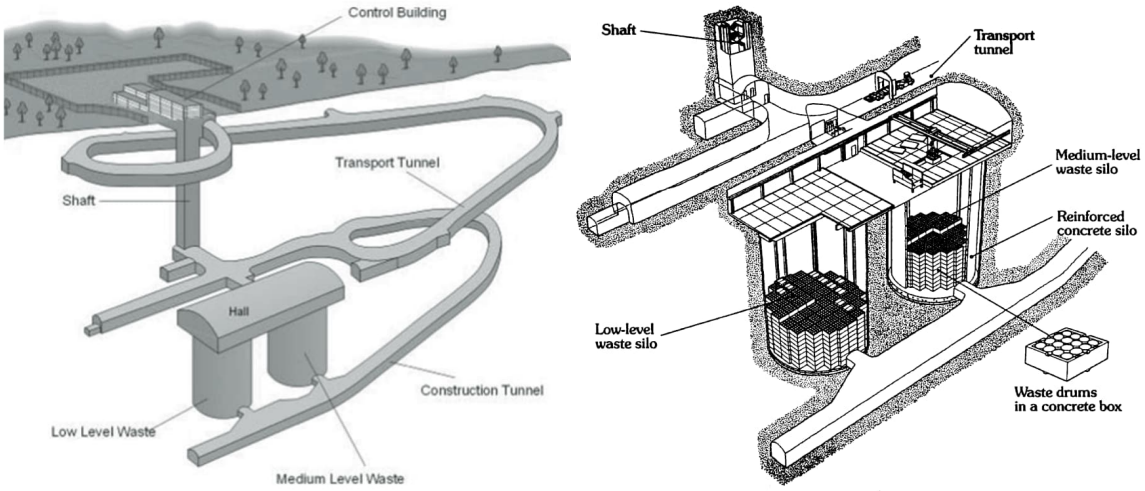

Figure 2. Schematic of the Olkiluoto VLJ Repository for LILW [5].

The construction of the LILW repository at the Olkiluoto site began in 1988 and operation began in 1992. The repository consists of two large silos (approximately 24 m ID x 34 m H) at a depth of 60 to 95 m in tonalite bedrock, one for solid LLW and the other for bituminized ILW. The silo for solid LLW is a shotcreted rock silo, while the silo for bituminized waste consists of a thick-walled concrete silo inside a rock silo where concrete boxes containing drums of bituminized waste are stacked. The repository is shown schematically in Figure 2.

At closure, the void space above the silos will be backfilled with local origin crushed rock. The reported waste inventory at VLJ was 5,681 m³ of LILW at the end of 2016 [6].The LILW from the new Olkiluoto 3 reactor will be disposed of in the same repository. The repository will be extended in the future with additional silos of similar design, to be able to receive all the waste from Olkiluoto 1, 2 and 3 reactors during the planned 60 years of operation of the units as well as for decommissioning waste.

1.3.2 Reinforced concrete rock vault concept

Concrete vaults are one of the most common methods used in the world today for disposal of LLW [7]. They are modular in nature, so can be scaled to a range of small to very large capacities and offer the flexibility to accept a wide variety of waste package sizes, including very large and heavy objects such as steam generators and reactor pressure vessels. They can also be constructed in a variety of geological settings at surface or near-surface at various depths up to several tens of meters. The basic vault consists of a thick-walled concrete

structure of various dimensions, often with a built-in drainage and/or water monitoring system. The concept of vault type repository has been implemented by Fortum at Loviisa.

Vaults are typically filled with waste packages from either the top (using a fixed or mobile crane) or side (using a forklift or similar vehicle), then covered with a concrete cap and engineered multi-layered cover system when full. Temporary weather covers can be used during the loading phase to protect the wastes and the structure and to minimize water ingress. Spaces between waste packages are typically backfilled with sand, gravel or concrete to form a monolithic structure prior to capping [5].

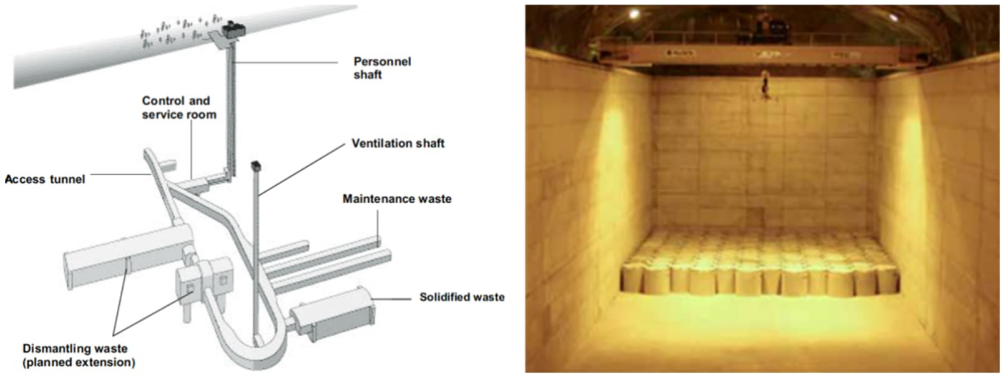

Figure 3. Schematic of Loviisa Repository for LILW [5].

At Loviisa, the construction of the repository was started in 1993 and the operation of the first phase of the disposal facility was started in 1998. As shown in Figure 3, the Loviisa repository is located at a depth of approximately 110 m in granite bedrock. The repository consists of waste halls for solid LLW ("maintenance waste") and a hall for solidified ILW.

The maintenance waste halls MWH1-2 have dimensions of 6 m W x 5 m H x 110 m long and have a waste capacity of 1200 m³ (or 6,000 drums). The halls have concrete floors and shotcrete walls with provisions for wall drainage. The waste drums are stacked five layers high within the tunnel. The LLW tunnels are not backfilled.

The reported inventory at Loviisa to end of 2016 was 1,886 m³ of LLW [6]. Inside the ILW cavern, the waste packages are emplaced in a basin made of reinforced concrete (approximately 70 m L x 14 m W x 11 m H). The vault will accommodate about 5,000 cylindrical concrete ILW containers (1 m³ each internal volume, 1.7 m³ external volume), stacked in 8 layers. The space between containers will be backfilled with concrete as each layer is filled and will be capped with concrete once filled. The space above the concrete basin will be filled with crushed rock.

1.4 Timeline of reinforced concrete deterioration

Concrete deterioration in repository conditions occurs over a very long time span, which can be in the order of thousands of years. During that time, the barriers must limit and retard the release of radionuclides effectively. The timeline for the deterioration of concrete in those conditions is divided according to the environmental conditions of the repository, which can affect the deterioration patterns that can occur during the lifespan of the barriers.

There are two main phases that the structure goes through in LILW repositories: the operation phase and the post-closure phase. LILW waste barriers must be able to safely store the deposited waste for a long service life, which can be in the order of thousands of years. The operation period lasts around 100 years. In this period, the concrete structure in the repository caverns is surrounded by air, and the waste is deposited into the containers inside the repository. Ensuring that the concrete barriers are in optimum condition by the end of this period is essential. It is recommended that the concrete mixture is chosen in a way that minimizes shrinkage cracks to make sure that the durability of the concrete is high. In cases where cracks develop, they must be repaired before the repository closure and the beginning of the post-closure phase.

The plants in both the Olkiluoto and Loviisa are in the operational phase. The plan for the repository in Loviisa is to be operational until the 2070s with the operating period extension of the Loviisa nuclear power plant. For Olkiluoto, the operation of the repository is planned to end in 2110s, and closure works ending by 2120s.

1.4.1 Repository operation phase

Typically, in LILW waste repositories, the operation period is estimated to be around 100 years. During this period, the facilities will be used, and the low and intermediate nuclear waste will be disposed of in the repository. Throughout this period, the underground caverns will be in contact with moist air. The average temperature in the underground repositories is estimated to be around 10 degrees Celsius, and the relative humidity is around 70%. The air in that environment also contains high carbon dioxide concentrations, which can be around 500 to 600 ppm. This high carbon content can lead to some changes to the concrete, such as carbonation, which changes the cement phases, and leads to reinforcement corrosion. The high humidity in the atmosphere can also act as a transport medium for other reactive agents

(sulfates and chloride for instance), but the effect of those chemicals from external sources is more of a concern in the post-closure phase.

During the operation phase, concrete deterioration can occur due to various drivers. The mix composition and mix materials of the concrete can be the reason for the deterioration of concrete (which continues into the post-closure phase). For example, the used aggregates in concrete can contain high sulfate and alkali content, which can be detrimental to the concrete. The existence of high sulfate content (which can be due to the addition of excessive gypsum or the use of contaminated aggregates) can result in ettringite formation, which can lead to expansion and cracking of the concrete. Alkali Silica Reaction (ASR) can also occur when the concrete has high alkali content, which reacts with aggressive silica in the aggregates to form an expansive material that leads to concrete damage.

The concrete can also be affected by carbonation in the operation phase. Carbonation normally occurs when concrete is exposed to the atmosphere. Carbon dioxide can penetrate through the concrete and alter some of its properties. Carbonation in the operation phase is important when considering a design for LILW repositories, due to the high CO_2 concentrations in the repositories and the higher humidity which can act as a driver for the carbonation process.

1.4.2 Repository Post-closure phase

In the post-closure phase, the caverns are closed, and they are gradually filled with groundwater. The concrete should be able to safely contain the waste for thousands of years. Throughout this phase, the water constantly flows into the concrete. The flowrate of the groundwater changes over time. The groundwater flow, as well as its composition, can alter the chemistry and morphology of the concrete. This alteration is very slow, but it can cause serious deterioration to the structure due to the long-life requirement of LILW repositories. The changes that occur to the concrete can - depending on the concrete and groundwater parameters – take hundreds or thousands of years to take effect.

The chemical composition of the groundwater greatly affects the deterioration mechanisms that occur to the concrete structure. Some of the ions that are present in groundwater can react with concrete and embedded reinforcement (if present), causing degradation and damage to the structure. Generally, the main chemicals that result in significant deterioration to the element are magnesium, sulfate, and chloride ions, which can interact with the concrete phases, causing damage to the concrete, or resulting in reinforcement corrosion. The cement

paste can also be leached out from the concrete over time, which weakens the concrete, and makes it more vulnerable to further degradation.

The groundwater that surrounds the concrete plays a large role in the degradation mechanisms affecting the structure. The chemical composition of the groundwater is dependent on the location of the barriers. Generally, the deeper the tunnel is, the lesser the purity of the groundwater in that location. The classification of the groundwater is done based on the Total Dissolved Solids (TDS), with higher solid content (and therefore, salts) in the water in deeper areas. In the Finnish repositories, the groundwater in the Olkiluoto has varying salinity.

Figure 4 [8] shows a chart of the timeline of both the operation and post-closure phases in LILW repositories. The deterioration mechanisms that affect the reinforced concrete in both of these phases according to the timeline are shown as well.

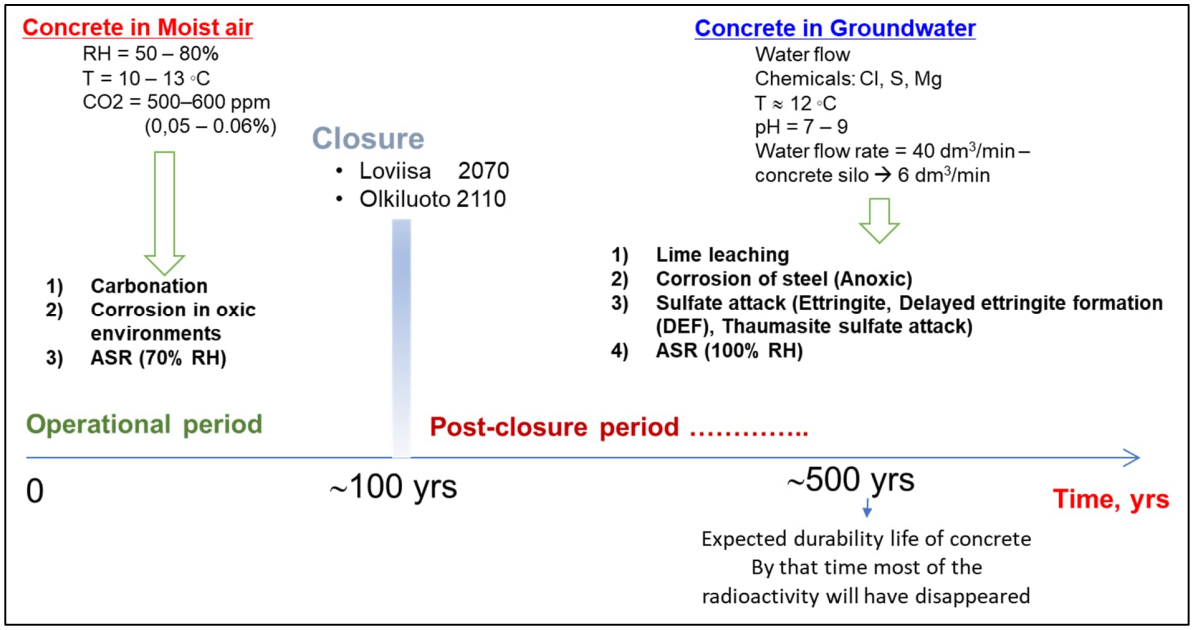

Figure 4. Timeline of the waste repository periods [8].

2. Ions and fluid transport mechanisms in concrete

Transport properties of concrete are a key factor for predicting their durability, since deterioration mechanisms such as corrosion, leaching or carbonation are all related to the ease with which a fluid or ion can move through the concrete microstructure. The passage of potentially aggressive species is primarily influenced by the penetrability of the concrete. Penetrability is broadly defined as the degree to which a material permits the transport through it of gases (e. g. nitrogen, oxygen and CO2 present in the atmosphere), liquids (e. g. water, in which various ions are dissolved), or ionic species. It embraces the concepts of permeability, sorption, diffusion, and migration/conduction and is quantifiable in terms of the transport [9], [10].

The processes involved in fluid and ion movement include the distinct mechanisms of:

1) capillary action,
2) fluid flow under pressure,
3) flow under a concentration gradient, and
4) movement due to an applied electric field.

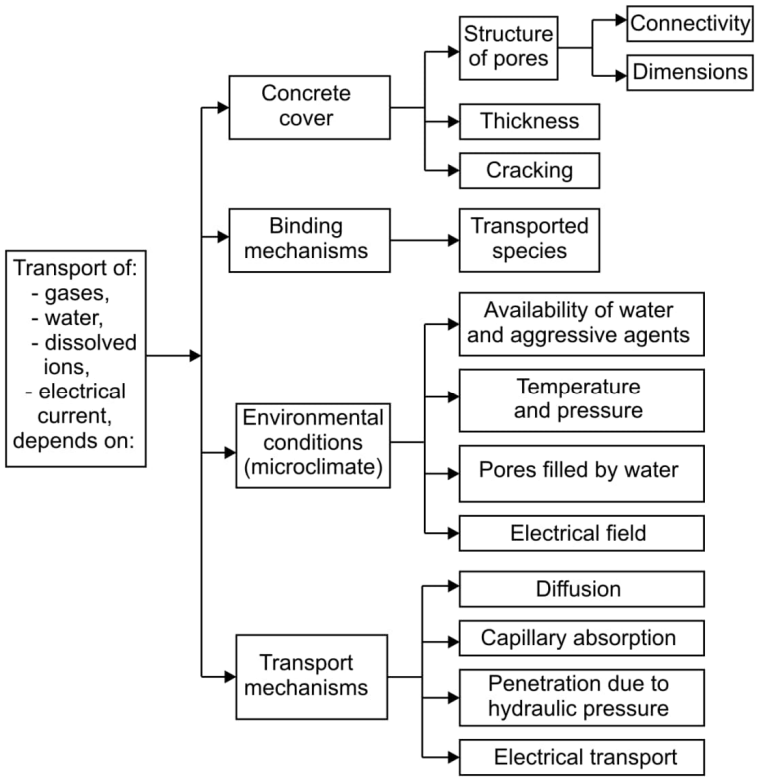

Figure 5. Principal factors involved in the transport processes in concrete [11].

The kinetics of transport depend on the mechanism, on the properties of the concrete (e. g., its porosity and the presence of cracks), on the binding by the hydrated cement paste of substances being transported, as well as on the environmental conditions existing at the surface of the concrete (microclimate) and their variations in time (Figure 5) [11].

2.1 Water vapour diffusion – due to concentration gradients

Diffusion is the movement of gases, ions and/or molecules under the influence of a concentration gradient, from an area of high concentration to one with a low concentration. Gaseous diffusion is experienced in unsaturated concrete while ionic diffusion occurs in saturated and partially saturated conditions. Molecular diffusion takes place if the pores of the medium are relatively large.

Stationary diffusion

The modelling of gaseous and ionic diffusion in concrete is commonly done using Fick's first law of diffusion (for stationary (steady) state diffusion – unidirectional and constant). This law may be used to describe the rate of diffusion of a gas/ion through a uniformly diffusable material.

$$J = -D_{eff} \frac{dC}{dx} \quad (1)$$

where J is the mass transport rate (g/m^{2}s), D_{eff} is the effective diffusion coefficient (m^2/s), dC/dx is the concentration gradient (g/m^3/m), C is the concentration of fluid (ion or gas, g/m^3) and x is the distance over which the diffusion occurs (m). The negative prefix denotes that the flux occurs along a negative concentration gradient.

Non-stationary diffusion

As diffusion rarely reaches stationary conditions in concrete structures, the flux depends on time t and is governed by Fick's second law:

$$\frac{\partial C}{\partial t} = D\frac{\partial^2 C}{\partial x^2} \tag{2}$$

This equation is usually integrated under the assumptions that the concentration of the diffusing ion, measured on the surface of the concrete, is constant in time and is equal to C_s ($C = C_s$ for x = 0 and for any t), that the coefficient of diffusion D does not vary in time, that the concrete is homogeneous, so that D does not vary through the thickness of the concrete, and that it does not initially contain chlorides (C = 0 for x > 0 and t = 0). The solution thus obtained is:

$$\frac{C(x,t)}{C_s} = 1 - \text{erf}\left(\frac{x}{2\sqrt{Dt}}\right) \tag{3}$$

Where the (erf) is the error function:

$$\text{erf}(z) = \frac{2}{\pi}\int_0^z e^{-t^2}dt \tag{4}$$

The values of the error function can be calculated by normal standard distribution, considering that:

$$\begin{gathered}\text{erf}(z) = 2N\left(z\sqrt{2}\right) - 1 \\ N\left(z\sqrt{2}\right) = \frac{1}{\sqrt{2\pi}}\int_{-\infty}^{z\sqrt{2}} e^{\frac{t^2}{2}}dt\end{gathered} \tag{5}$$

Diffusion acts as a predominant degradation mechanism for concrete structures fully submerged in sea water or salt-contaminated soil. In combination with other mechanisms, diffusion contributes to chloride transport in concrete under most exposure conditions. The transport of oxygen in concrete to the steel surface is also governed mainly by diffusion process. The rate of diffusion of oxygen is determined by the pore structure, pore size

distribution of concrete and its moisture content. It decreases sharply with the increase in moisture content [9].

2.2 Permeation mechanism – due to pressure gradient

Permeability of concrete is defined as a measure of the capacity of concrete to transfer fluids through its pore structure under an externally applied pressure whilst the pores are saturated with that fluid. The driving force for liquids and gases through the pore spaces or crack networks is a pressure gradient. For permeation, Darcy's law is used to calculate average velocity of flow of the fluid ($\bar{v}$):

$$\bar{v} = \left(\frac{k}{\phi}\right)\left(-\frac{dh}{dx}\right) \tag{6}$$

where k is the permeability coefficient, ϕ is the porosity of concrete, h is the hydraulic pressure head and x is the distance.

Permeation plays an important role in water retaining structures where water transport through the structure is detrimental.

2.3 Sorption by capillary suction

Sorption refers to uptake of liquids into an unsaturated or partially saturated solid by capillary suction. It is measured using parameters such as bulk absorption, or sorptivity (S). Sorptivity is essentially the movement of a wetting front in a dry or partially saturated porous medium:

$$S = \frac{\Delta M_t}{t^{1/2}}\left[\frac{d}{M_{sat} - M_0}\right] \tag{7}$$

where $\left(\Delta M / t^{1/2}\right)$ is the slope of the straight line produced when the mass of water absorbed is plotted against the square root of time, d is the sample thickness, ($M_{sat}\ and\ M_o$) are the saturated mass and dry mass of concrete specimen respectively.

Sorptivity is influenced by the larger capillaries and their degree of continuity and is very sensitive to hydration of the outer concrete surface, and, hence curing. It is also influenced by compaction and aggregate orientation and distribution and by the mix composition.

2.4 Convection as a result of the bulk moving water

Convection (or advection) is the process that describes the transport of a solute (e.g., chloride or sulphate ions) as a result of the bulk moving water [9]. The process is described by:

$$\frac{\partial C}{\partial t} = -\bar{v}\,\frac{\partial^2 C}{\partial x^2} \tag{8}$$

where C is the concentration of solute at depth x after time t and $\bar{v}$ is the average velocity vector of fluid flow.

Convection (together with diffusion) is the main transport mechanism for chloride ingress in cracked concrete [9]. It also has an important role in the movement of chloride ions when concrete is exposed to drying-wetting conditions.

2.5 Water transport due to wick action through concrete

Wick action is the transport of water and the ions it may contain through a concrete structure from a face in contact with water/salt solution to a drying face (Figure 6). It may also occur in concrete exposed to wetting and drying cycles. Wick action is often dominated by convection. Chlorides can penetrate concrete by wick action. It results in a build-up of chlorides inside the concrete particularly near the drying face.

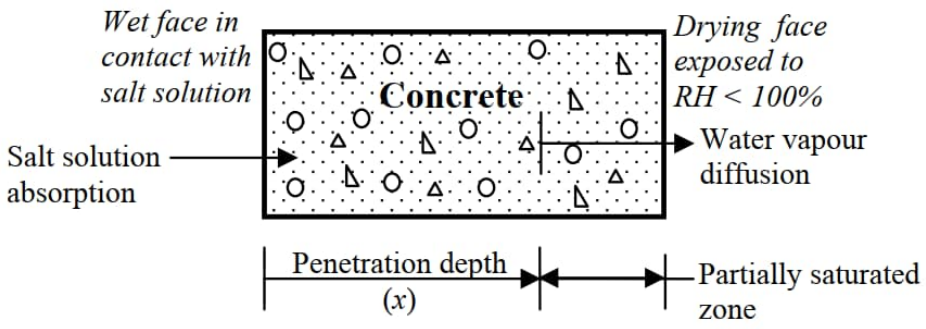

Figure 6. A schematic illustration of wick action in concrete [11].

3. Modelling of the concrete deterioration in waste repositories

The process of concrete deterioration in repository barriers occurs over a long period of time, during which, the barriers must be able to resist the environmental and internal degradation for over period of thousands of years The processes of the deterioration, which include leaching, sulfate attacks, and changes to the microstructure of the material takes a long time and depend on different variables such as the concrete mix, the design of the barriers, the flowrate and composition of the groundwater, and so on. Experiences of concrete structures are limited compared to that time, which amplifies the need for simulation endeavors for establishing information on the potential deterioration and concerns in such structures.

One of the key aspects in concrete modelling is to understand how the concrete phases change and interact with its environment. The mineralogy of concrete, along with its physical properties play a large role in its response to outside agents, which was discussed in the previous chapter. Conventional models have the aim of predicting the performance of a concrete mixture under different conditions. In repository conditions, the models aim to investigate the concrete's long-term performance in different conditions that relate to its composition (which can include the addition of mineral admixtures), the composition of groundwater, the hydration of concrete, the interaction between the mixture and the surrounding environment (sulfate, magnesium, and chloride ions, as well as the leaching of the cement paste).

In this chapter, a review of different reports regarding the modelling of concrete in repository conditions is done. This chapter also discusses some of the shortcomings present in the use of numerical models for assessing the performance of structures in repository conditions, as well as the possible future trends and opportunities that can improve the reliability of conceptual models.

For developing conceptual models, the processes and interactions between concrete and groundwater are important to foresee the possible changes in the barrier. The chemicals in the groundwater can react with the cement phases, producing different chemicals that can have different properties. The changes in the concrete's mineralogy can also influence its interaction with the flowing groundwater. The aim of conceptual models that simulate concrete deterioration is to assess and quantify the chemical processes, dissolution of cement phases, and ion exchange in the matrix to examine the changes occurring to the concrete in a certain environment.

3.1 Deterioration mechanisms of concrete

Durability modelling of reionforced concrete requires an understanding of the mechanisms involved in the time-dependent progress of concrete deterioration and reinforcement corrosion. Deterioration mechanisms of reinforced concrete are divided into (i) chemical and (ii) physical deterioration mechanisms [12]. The chemical and physical deterioration mechanisms may be divided into those concerning the corrosion of the reinforcement and those affecting the concrete. The reinforcement degradation may be caused by: (i) carbonation of concrete and (ii) ingress of chlorides into concrete. The progress of corrosion of the reinforcement eventually leads to possible failure modes such as bond loss, loss of steel cross-section and loss of concrete cover due to cracking and spalling of concrete. The physical and chemical mechanisms of deterioration for reinforced concrete can be categorized as shown in Figure 7.

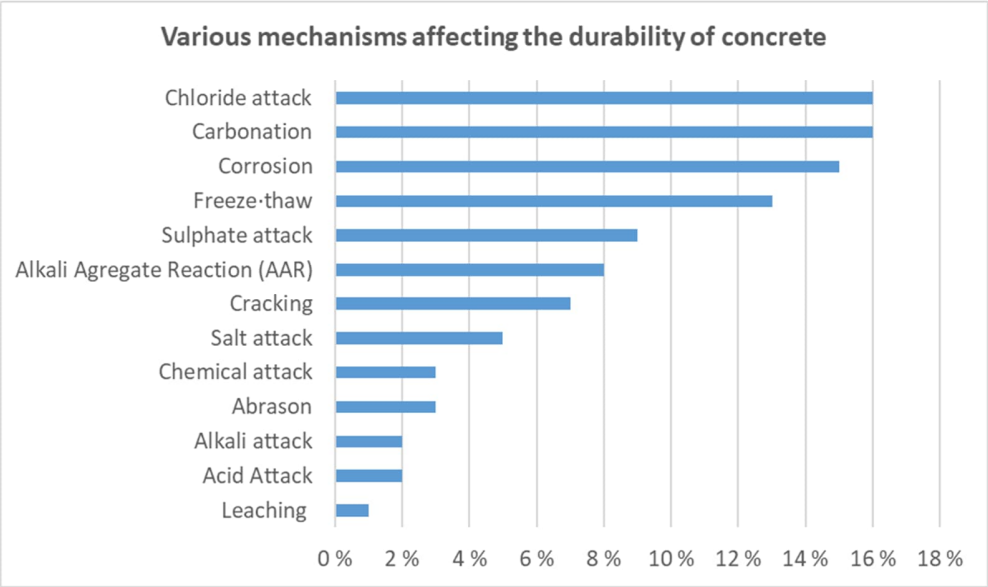

Figure 7. Reference to percentages assigned to the contribution of various mechanisms affecting the durability of concrete structures (Review of more than 400 published documents on deterioration of concrete, during 1980 – 2000) [13].

Since the deterioration of concrete is subject to more numerous effects, an examination of the macro- and micro-environment of the system in conjunction with the structural requirements is needed to describe the causes of such deterioration. The mechanisms of deterioration and their rate are controlled by the environment, the paste microstructure and the fracture strength of concrete. The relevent environmental factors that affect the reinforced concrete in LILW reporistories include concentration of deleterious chemicals in the ground and the groundwater.

The deterioration mechanisms of reinforced concrete structures can be explained as presented in Figure 8 [13]:

1) The microstructure of concrete is controlled by:
   a) Constituent materials and their mix proportions in the concrete mix: properties of cement, aggregate and sand; admixtures and cement replacements; quality of water; etc.,
   b) Method of manufacturing concrete: mixing, transporting, placing, compacting and finishing the concrete,
   c) Subsequent treatment of the concrete: curing, surface treatments, age of exposure to load and service conditions, etc.
2) The ingress of aggressive agents depends on the various moisture transport processes, i.e. diffusion, absorption and permeability, and one or more of the deterioration mechanisms are influenced by the transport of these deleterious agents through concrete.
3) The various mechanisms of deterioration which are either influenced by the transport or the different aggressive substances are corrosion of reinforcement, freeze-thaw damage, salt attack, or Alkali-Silica Reaction (ASR), sulphate attack and acid attack. Both acid attack and ASR are not influenced by the transport mechanisms within the concrete; however, their damage in concrete depends on the permeation properties of concrete.
4) As deterioration progresses, concrete cracks. The ultimate result of the permeation of deleterious materials into concrete is therefore cracking and spalling of the cover concrete in reinforced concrete structures. Cracks (both micro and macro) facilitate the ready penetration of various chemicals into the concrete resulting in the acceleration and progression of deterioration. Thus, cracking influences the permeation properties which in turn aggravate deterioration.

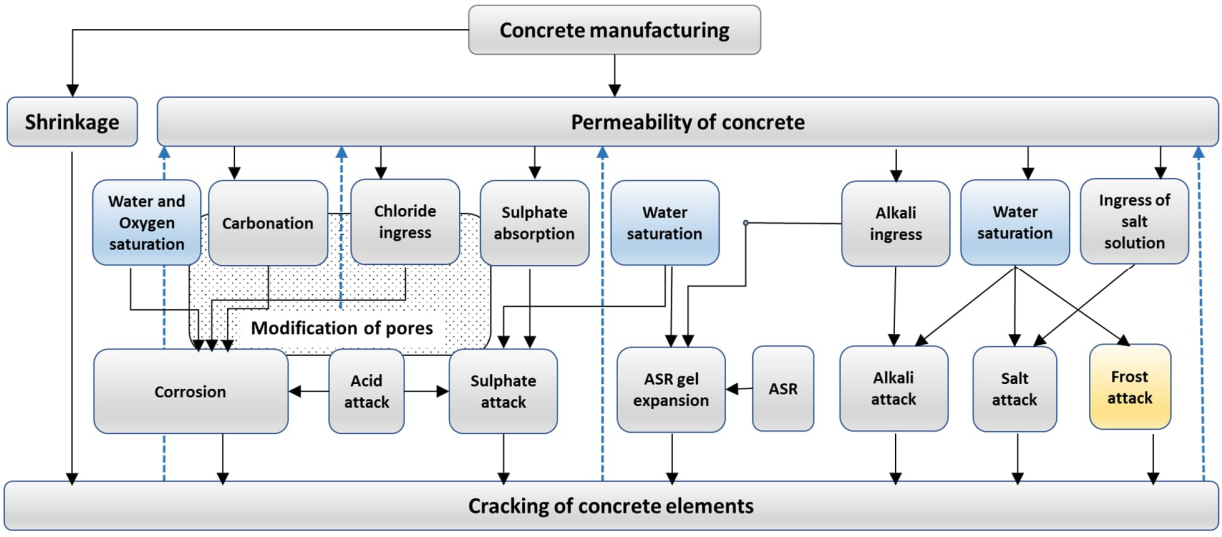

Figure 8. Causes of deterioration - permeability interaction model [13].

Concrete deterioration can occur in waste repositories by various mechanisms. The affecting mechanisms result in changes to the concrete phases, which can deteriorate the concrete, cause an imbalance to its equilibrium, or result in the corrosion of the embedded reinforcement bars.

3.2 Carbonation of concrete

In LILW repositories, carbonation of concrete is a concern during the operation phase of the NPP, during which the atmospheric environment in the repositories typically contain high CO_2 levels, as well as high humidity which can speed the rate of ion transport through the concrete.

3.2.1 Mechanism of carbonation induced corrosion

Carbonation is the combination of physical and chemical concrete transformations under the influence of prolonged exposure to carbon dioxide. Carbon dioxide is always present in ambient air and the internal atmosphere of buildings. In the atmosphere, the concentration of CO_2 by volume is about 0.04%, but in industrial areas or along the roads may be 0.3% and locally even more, so in the concrete with surface uncovered with other the material carbonation process runs continuously. The main causative mechanism of carbonation is the reaction of atmospheric CO_2 with calcium hydroxide, one of the cement hydration products (Figure 9). The products of this reaction are calcium carbonate and water [14].

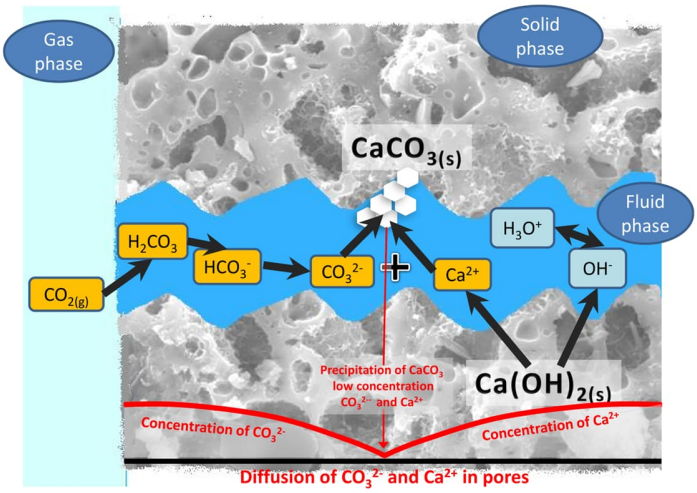

Figure 9. Mechanism of carbonation [14].

The carbonation process is time dependent, and it slows down considerably with higher depth. Carbonation has an inverse relationship with time, and it slows down exponentially, which is shown in Figure 10. The carbonation rate is also heavily dependent on the humidity level of the concrete's environment, with insignificant carbonation below 25% relative humidity, and no carbonation activity in submerged concrete (which makes carbonation only a concern in the operation period in repository conditions). In the operation phase in LILW repositories, the relative humidity is around 65%, and that is in the optimum range for carbonation activity [15].

Carbonation in the concrete starts when CO_2 ions enter the concrete structure, which is largely dependent on the concrete's microstructure and porosity. The CO_2 enters through the concrete's matrix, and then it reacts with $Ca(OH)_2$ in the cement phases. The result of this reaction is calcium carbonates, or calcite ($CaCO_3$). The reaction is shown in equation (9). Due to this reaction, the concrete's alkalinity is reduced, from 13 pH to around 8.5 pH. The changes to the concrete are gradual, starting from the surface of the concrete, and increasing in depth.

The mechanism of carbonation is the reaction of diffused CO_2 with calcium hydroxide. The final products of this reaction are $CaCO_3$ and water. The physicochemical processes involved in carbonation are [16], [17]:

1) The diffusion of CO_2 in the gaseous phase of the concrete pores.
2) The dissolution of CO_2 in the pore water as carbonic acid.
3) Dissociation of CO_2 as H_2CO_3 and CO_3^{2-} ions.
4) The dissolution of solid $Ca(OH)_2$.
5) Releasing calcium Ca^{2+} and hydroxyl OH^- ions.
6) The precipitation of Ca^{2+} with CO_3^{2-}, forming $CaCO_3$

1. Solvation: $CO_{2(g)} \rightarrow CO_{2(l)}$
2. Reaction: $CO_{2(l)} + H_2O_{(l)} \rightarrow H_{2CO_{3(l)}} \rightarrow H^+ + HCO_3^- \rightarrow 2H^+ + CO_3^{2-}$
3. Hydration: $CaO_{(s)} + H_2O_{(l)} \rightarrow Ca(OH)_{2(s)}$ (9)
4. Ionization: $Ca(OH)_{2(s)} \rightarrow Ca^{2+} + 2OH^-$
5. Precipitation: $Ca^{2+} + 2OH^- + 2H^+ + CO_3^{2-} \rightarrow CaCO_{3(s)} + 2H_2O_{(l)}$

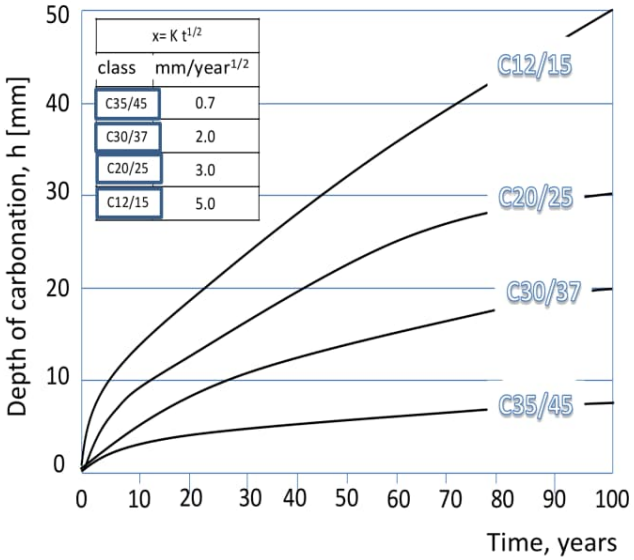

Figure 10. Typical carbonation depth pattern for different concrete strength classes, slowing down with time based on [18].

In reinforced concrete structures, reinforcement bars are protected from corrosion by a protective layer of the concrete. This protective layer works due to the high alkalinity of concrete. When the alkalinity of the concrete structure around the depth of the embedded reinforcement is reduced beyond a certain point (around 9.5 pH), the passive protective layer is depleted, and corrosion of the reinforcement due to carbonation can commence.

Carbonation is divided into two stages: i) the initiation stage and ii) the propagation stage. The initiation of carbonation begins when CO_2 enters the microstructure of concrete and reacts with the $Ca(OH)_2$. The propagation stage starts when the carbonation depth reaches the depth of reinforcement, marking the depletion of the passive layer leading to the start of carbonation-induced corrosion.

Carbonation leads to changes in the cement phases, reducing the alkalinity of concrete, and corroding the embedded rebars. Due to reinforcement corrosion, the volume of the rebars is increased. This volumetric expansion causes internal stresses inside the concrete, which can lead to loss of bond between the rebars and concrete, cracking and spalling of material. The corrosion pattern that occurs due to carbonation is uniform. Carbonation, as a phenomenon, occurs at a somewhat uniform rate, leading to a uniform corrosion pattern. Figure 11 shows a rebar section that exhibits uniform carbonation-induced corrosion.

Figure 11. Uniform corrosion due to carbonation.

By the end of the operation period in LILW repositories, the caverns are closed off, and groundwater gradually surrounds the concrete. This creates an anoxic environment, which slows down corrosion rates of rebars. Additionally, carbonation does not occur in submerged concrete, which makes carbonation of concrete insignificant in the post-closure phase in LILW repositories.

3.2.2 Modelling of the carbonation of concrete in the operation phase

Carbonation of reinforced concrete changes the cement phases (forming calcite), reducing the alkalinity of concrete, and it can lead to the corrosion of the embedded reinforcement bars. The carbonation phenomenon is known to slow down with time. In waste repositories, carbonation is only a matter of concern during the operation period. During the post-closure period, where the concrete is in a saturated anoxic state, carbonation becomes negligible. Therefore, the carbonation progression is typically not considered after the end of the operation period.

A traditional expression based on Fick's law that is used to predict the carbonation of concrete, where carbonation is determined as the squared root of time, is shown in equation (10):

$$x = k \cdot \sqrt{t} = \sqrt{\frac{2D\varphi_{ext}}{a}} * \sqrt{t} \qquad (10)$$

Where x is the carbonation depth, t is the time, and k is a parameter that reflects the carbonation rate, D is the diffusion coefficient m^2/s and φ_{ext} is the CO_2 concentration in the air. a is the coefficient determining the amount of CO_2 bound in the way of carbonation by unit volume of concrete in kg/m^3, calculated according to the Bulletin CEB [19] as:

$$a = 0.75 \cdot C \cdot [CaO] \cdot \alpha_H \cdot \frac{M_{CO2}}{M_{CaO}} \tag{11}$$

wherein the C is the content of cement, kg/m^3; $[CaO]$ is the CaO content in the cement composition; α_H – the degree of hydration of cement; $M_{CO2}\ and\ M_{CaO}$ are the molar masses of CO_2 and CaO.

Also a formula in the following form is often used for estimating the carbonation depth:

$$x = \sqrt{\frac{2D \cdot t \cdot [CO_2]}{[Ca(OH)_2]}} \tag{12}$$

where $[CO_2]$ and $[Ca(OH)_2]$ are the molar concentration of carbon dioxide and calcium hydroxide concentration, D is the diffusion coefficient and t is the time of exposition.

Equation (10) and Equation (12) are a significant simplification of the description of the process of carbonation, which does not take into account a number of additional factors, such as changes in diffusivity as a function of humidity, changes in atmospheric concentrations of CO_2 in climatic year, participation in the carbonation of CSH phase and residuals of non-hydrated cement, qualitative and quantitative characteristics of the material composition of concrete (w/c, type of cement, additives, admixtures), technological and environmental factors (curing, temperature, state of stress) and first of all diffusivity changes resulting from changes in time of the concrete microstructure [19].

Examples of the modification of the basic model (Equation (12)) when taking into account the material variables, technological and environmental factors are presented below. Al-Neshawy [20] suggested a model of the time-dependent carbonation depth of concrete. The carbonation depth model takes into consideration the effect of the composition of the concrete and the history of the relative humidity and temperature on the carbonation depth of concrete.

$$X_{\mathrm{ca}} = k_{\mathrm{con}} * k_{\mathrm{cur}} * k_{\mathrm{T}} * k_{\mathrm{RH}} * k_{\mathrm{CO_2}} * \sqrt{t} \tag{13}$$

Where, k_{con} is the quality of concrete related coefficient, k_{cur} is the concrete curing factor, k_{RH} is the relative humidity related coefficient, k_T is the temperature related coefficient, and k_{CO2} is the square root of the carbon dioxide content in air.

Papadakis [21] summarised the main composition parameters of concrete that affect the carbonation process as the water-to-cement ratio and aggregate-to-cement ratio. A simplified expression of the effect of the composition of the concrete on the depth of the carbonation with time is shown in Equation (14).

$$k_{\mathrm{con}} = 350 * \frac{\rho_c}{\rho_w} * \left(\frac{\frac{w}{c} - 0.3}{1 + \frac{\rho_c}{\rho_w} * \frac{w}{c}} \right) * \sqrt{1 + \frac{\rho_c}{\rho_w} * \frac{w}{c} + \frac{\rho_c}{\rho_a} * \frac{a}{c}} \quad (14)$$

Where, ρ_c is the mass density of the cement [kg/m³], ρ_w is the density of the water [kg/m³], ρ_a is the mass density of the aggregates [kg/m³], *w/c* is the water-to-cement ratio [-], and *a/c* is the aggregate-to-cement ratio [-].

According to Duracrete [22], [23], the values of the concrete curing coefficient (k_{cur}) for the carbonation resistance are 1.0 for 7 days' curing and 0.76 for 28 days' curing of the concrete. The influence of the ambient temperature history of the concrete surface on the carbonation depth is shown in Equation (15) [24].

$$k_{\mathrm{T}} = EXP\left(\frac{Q}{R} * \left(\frac{1}{273 + T_0} - \frac{1}{273 + T} \right) \right) \quad (15)$$

Where, *Q* is the activation energy of the carbonation process, *Q* = 2.7 [kJ/mol], *R* is the gas constant, *R* = 0.008314 [kJ/mol.K], T_0 is a reference temperature, T_0 = 25 [°C] and *T* is the actual temperature in the concrete [°C].

Kari [24], quantified the effect of the history of the ambient relative humidity on the carbonation depth of the concrete according to Equation (16).

$$k_{\mathrm{RH}} = \left(1 - \frac{RH}{100}\right)^n \; for\; RH \geq 65\% \quad (16)$$

Where, *RH* is the relative humidity in the concrete cover [%], and *n* is an exponent of range (1 – 2.5). The value of the exponent (*n*) is considered to be 1.1 on the basis of comparing the model results with the natural carbonation depth results.

The carbonation process has an ongoing need for carbon dioxide from the atmosphere. The carbon dioxide content of the atmosphere by volume is considered to be 0.035% (350 ppm) and the value of k_{CO2} is considered to be 0.0187.

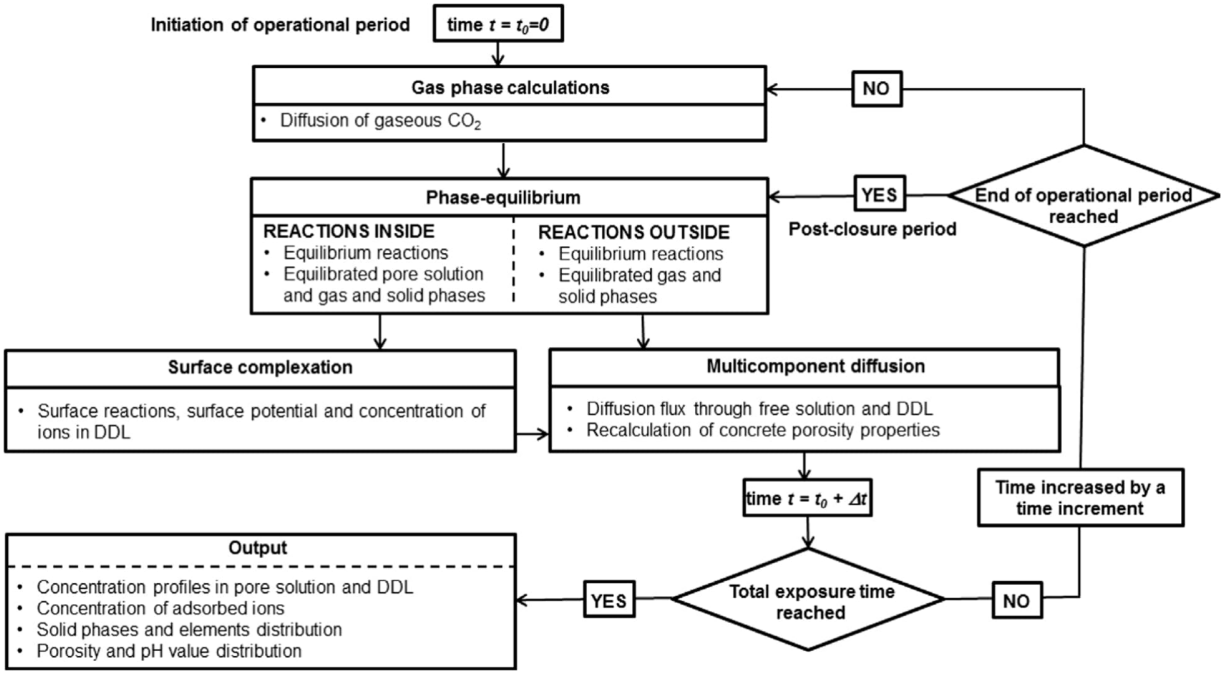

Figure 12. Flow chart of the thermodynamical model [25].

Kari [24]–[28] presented a thermodynamical model for simulation of concrete carbonation in Finnish rock cavern conditions for final disposal of nuclear waste. The atmospheric carbon dioxide diffuses into concrete in gaseous phase, where it dissolves into pore water. The carbonation related phenomena change the properties of concrete. The thermodynamical model consists of (i) phase-equilibrium, (ii) surface complexation and (iii) multicomponent diffusion modules. The model was implemented in geochemical PHREEQC software [29]. Basic structure of the calculation procedure is presented in Figure 12. The main governing equations are also presented next [25].

1) Gas phase calculations

The diffusion of gaseous CO2 is given as:

$$D_{gCO_2} = D_{g0} \cdot \tau \cdot (1 - \varepsilon) \tag{17}$$

where D_{g0} is the diffusivity of CO_2 in free atmosphere [$1.34 \times 10^{-5}\ m^2/s$], τ is the tortuosity factor [–], and ε is the water filled porosity [–].

The diffusivity is assumed to be the same in free atmosphere and in air-filled pores. The degree of pore volume saturated by the pore solution is defined as a constant depending directly on the prevailing relative humidity taking also into account the water produced by carbonation.

In general, the partial pressure of a gas component may be written in terms of aqueous phase activities as follows:

$$P_g = K_g^{-1} \cdot \prod_i (\gamma_i \cdot C_i)^{n_{i,g}} \tag{18}$$

where P_g is the partial pressure of gas component g calculated using activities in the aqueous phase [atm], K_g is the Henry's law constant for the gas component [atm], γ_i is the activity coefficient of ion i [–], C_i is the concentration of ion i [mol] and $n_{i,g}$ is the stoichiometric coefficient of master species in the dissolution equation [–].

2) Phase-equilibrium

The phase equilibrium calculations are used to define the amount of cement hydrate phases that can react reversibly with an aqueous solution to achieve equilibrium. The phases will dissolve or precipitate to achieve the equilibrium or will dissolve completely. The equilibrium reactions are expressed by the mass-action equations. In general, the pure phase equilibrium can be written as:

$$K_p = \prod_i (\gamma_i \cdot C_i)^{n_{i,p}} \tag{19}$$

Where K_p is the thermodynamic equilibrium constant for the phase p [–], γ_i is the activity coefficient of ion i [–], C_i is the concentration of ion i [mol], and $n_{i,p}$ is the stoichiometric coefficient of ion i in the phase p [–].

3) Surface complexation reactions

The adsorption of ions on the charged surface of the pores, which mainly means the adsorption of calcium, is modelled through surface complexation reactions. The generalised two-layer surface complexation model, built in PHREEQC, explicitly calculates the composition of the diffuse layer. The surface charge density σ (sites/nm^2) is the amount of charge per area of the surface, as follows:

$$\sigma = \frac{F}{A \cdot S} \cdot [(\equiv XOH_2^+) + (\equiv XOM^+) - (\equiv XO^-) - (\equiv XOA^-)]$$
$$\sigma = F \cdot \left[\Gamma_H - \Gamma_{OH} + \sum (Z_M \cdot \Gamma_M) + \sum (Z_A \cdot \Gamma_A)\right] \quad (20)$$

In the equation F is the Faraday constant (C/mol), A is the specific surface area (m^2/g), S is the solid concentration (g/L), and Z is the valence of an adsorbing ion (+/-). The adsorption densities (mol/m^2) are presented by the symbol (Γ). Symbols Γ_H and Γ_{OH} represent the adsorption densities of protons and hydroxide ions, respectively, whereas Γ_M and Γ_A are used for adsorbed cations and anions in the process.

The Boltzmann distribution, the net charge density (σ) at a distance x (m) from a charged surface can be written:

$$\sigma(x) = \sum_{i=1}^{n} z_i \cdot F \cdot C_i \cdot EXP\left(\frac{-z_i \cdot F \cdot \psi(x)}{RT}\right) \quad (21)$$

Where ψ is the electrical potential (V) at a distance x from the adsorbed layer, z_i is the charge number [–] and C_i is the molar electrolyte concentration (mol) of ion i. In the common case, where the electrical field is generated by a charged flat surface (such an electrode), Equation (21) can be rewritten as the Poisson–Boltzmann equation:

$$\frac{d^2\psi(x)}{dx^2} = -\frac{\sigma(x)}{\varepsilon_0 \cdot \varepsilon} = -\frac{F}{\varepsilon_0 \cdot \varepsilon} \cdot \sum_{i=1}^{n} z_i \cdot C_i \cdot EXP\left(\frac{-z_i \cdot F \cdot \psi(x)}{RT}\right) \quad (22)$$

Where ε is the dielectric constant of water (–) and ε_0 is the permittivity of free space equal to 8.854×10^{-12} (C/Vm). The model used for its derivation is called the Gouy-Chapman theory, which is assumed for the ionic distribution in the diffuse layer.

4) Multicomponent diffusion (MCD)

The multi-component diffusion in liquid phase is simulated through a charge-free pore solution and the Diffuse Double Layer (DDL). The diffusive flux J_i [mol/m2/s] of an ion i in a solution as a result of chemical and electrical potential gradient is expressed as:

$$J_i = -\frac{u_i \cdot C_i}{|z_i| \cdot F} \cdot \frac{\delta \mu_i}{\delta x} - \frac{u_i \cdot z_i \cdot C_i}{|z_i|} \cdot \frac{\delta \psi}{\delta x} \quad (23)$$

where u_i is the mobility of ion i in water [m2/s/V], z_i is the charge number [–], μ_i is the electrochemical potential [J/mol], and ψ is the electrical potential [V].

The diffusive flux can be used for both charge-free solution and DDL. Only the concentrations of ions are different in charge-free solution and DDL. The gradient of electrical potential $\delta\psi/\delta x$ originates from different transport velocities of ions, which creates charge and an associated potential.

3.3 Chloride ingress

Chloride ingress in concrete structures can have a great influence on their behavior throughout its functional life, especially in reinforced concrete. Chloride ions can penetrate the concrete matrix (mainly with water, but it can enter with moisture as well), resulting in the breakdown of the oxide passive layer that protects the embedded reinforcement bars, and subsequently leading to corrosion of rebars and subsequent cracking of the reinforced concrete element.

3.3.1 Chloride interaction with hydrated cement systems

Typically, chlorides can attack concrete from external sources. Chlorides can be present in the concrete's environment (for example, in sea water, groundwater, de-icing salts, and moisture), and through that medium, they can penetrate into the concrete matrix. Chloride penetration can occur by different mechanisms, with diffusion being the most common

method. Chlorides can also be transported into the concrete by other mechanisms, such as convection and absorption. The diffusion of chloride into the concrete in complete saturation is governed by Fick's second law, which shows the chloride content, the diffusion coefficient, as well as the time and distance. Chloride ingress can be affected by various factors, such as the concrete mix, porosity, the chloride concentration in the exposure medium, the saturation degree of the concrete, and so on.

As discussed previously in the carbonation-induced corrosion part, the concrete forms a passive layer around the rebar, and that passivity can act as a shield that protects the embedded reinforcement surrounded by it. Chlorides can, however, attack this passive layer directly, which makes them 'override' the pH reduction requirement that was previously needed for carbonation-induced corrosion. When enough chloride ions reach the reinforcement depth, the propagation stage of chloride-induced reinforcement corrosion begins. Because the penetration of chloride ions is not uniform (unlike carbonation, which is somewhat uniform), the rebars show a different corrosion pattern known as pitting corrosion. When enough chloride ions (which is known as the threshold limit) reach the rebar depth in reinforced concrete, the reaction that causes chloride-induced corrosion starts leading to local pitting in the rebar that subsequently causes cracking and delamination of the reinforced concrete, as well as a breakdown to the rebar. Figure 13 shows chloride-induced corrosion in a reinforcement bar.

Figure 13: Pitting corrosion in an embedded rebar.

Chloride ingress in the concrete matrix typically follows a pattern that is depicted in Figure 14. The chloride ions at the edges of the concrete are high, and they decrease gradually with the increase in depth into the concrete. The outer edge of the concrete may have slightly lower chloride content, which is mainly because chlorides can get flushed out with water in the far edges. Due to the 'simple' nature of the figure, incorrect assumptions can be made when the kinetics of chloride attack are studied.

The chloride threshold is the chloride content level at which they start attacking the passive layer of the concrete, and therefore initiating the chloride-induced corrosion. This threshold limit varies based on different factors, such as the environment surrounding the concrete. Humidity, moisture, and oxygen content play a large role in determining this threshold limit. In submerged concrete in anoxic environments, corrosion activity becomes limited, which results in an increase in the required threshold limit that initiates chloride-induced corrosion. This threshold limit typically ranges between 0.4 – 3% per weight of the cement (0.4% is typically a conservative limit in some codes), depending on the environment of the concrete (with differences in humidity, cycles of wetting and drying, etc.), with submerged concrete members having a chloride threshold limit of around 2.5% according to some studies [30].

Chlorides can react with the hydrated and anhydrous cement phases (mainly aluminates), resulting in the formation of other solid phases, such as Friedel's salt ($C_4ACl_2H_{10}$). Friedel's salt is a solid chloride phase, which is considered bound to the concrete. This phase is rather ambiguous, as it can solidify in the concrete pores, which can be somewhat positive as it slows down the ingress of chemicals into the concrete, but the effects of Friedel's salt on the durability of concrete are still an area of debate. Generally, chlorides in the form of Friedel's salt are bound in the concrete, which reduces the porosity of the concrete, and reduces the "free" chlorides in the system, which can, to some extent, slow down expansive aluminate consumption, bind some of the chlorides to the concrete matrix, and reduce the chloride ingress around the rebars (either by being physically bound, or by reducing concrete porosity [31], [32].

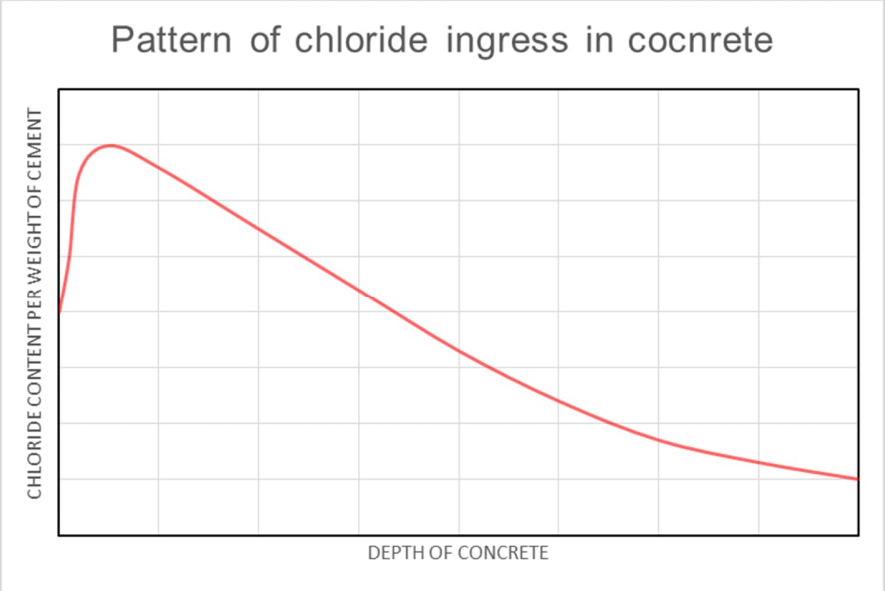

Figure 14: The typical pattern for chloride ingress in concrete, showing a peak just beyond the concrete edge.

The interaction between chlorides and sulfates becomes even more complex when considering chloride binding and Friedel's salt. As mentioned before, sulfate ions interact with the aluminate phases in the cement paste, which results in the creation of ettringite. Friedel's salt forms when chlorides interact with aluminates as well. The formation of either ettringite or Friedel's salt can block the pores in the concrete, slowing the ingress of chlorides and sulfates into the concrete. Chlorides and sulfates are also competing for aluminates in the concrete phases, which can affect the interactions inside the concrete.

Groundwater in LILW repositories contain chloride ions. The concentration of chlorides varies depending mainly on the depth of the repository. The presence of chloride ions can pose the risk of reinforcement corrosion during the lifespan of the structures. In some cases, engineered barriers are designed with no embedded reinforcement to avoid the risk of chloride induced corrosion. This becomes more of a consideration in locations that have groundwater with high salinity, which further increases corrosion risks. In Finland, however, the LILW repositories are made with reinforced concrete.

3.3.2 Modeling chloride ions ingress

Traditionally, Fick's 1st law has been used to describe the chloride flux as a result of pure diffusion in liquid water, with the concentration c of dissolved chloride as the transport potential [33].

$$q_{Cl} = -D_{F1}\frac{dc}{dx} \tag{24}$$

1) Basic model of chloride ion transport

The classical Fick's second law is used to calculate the relationship between the concentration of the diffusion medium at a certain depth and time. The mathematical expression is:

$$\frac{\partial C}{\partial t} = D \cdot \frac{\partial^2 C}{\partial x^2} \tag{25}$$

where C is the volume mass of diffusion material (kg/m^3), D is the diffusion coefficient (m^2/s), t is the diffusion time (s) and x is the diffusion distance (m).

First, a reasonable assumption for concrete is made, and then combined with Fick's second law to obtain a relatively accurate chloride ion transport model, which can be used to calculate the life cycle of concrete. The basic assumptions are as follows [34]:

1) The concrete is semi-infinite, and the medium is uniform.
2) The diffusion of chloride ions in concrete is one-dimensional.
3) The chloride ion does not adsorb and combine with the substances in the concrete, that is, the chloride ion binding capacity of the concrete is 0.
4) The chloride diffusion coefficient is constant.
5) The chloride concentration exposed to the concrete surface is constant.

Based on the above assumptions, the diffusion equation of chloride ions in concrete is obtained:

$$C(x,t) = C_i + (C_s - C_i)\left(1 - \mathrm{erf}_{(x)}\left[\frac{x}{2\sqrt{D_{nss} \cdot t}}\right]\right) \tag{26}$$

Where $C(x,t)$ is the content of ion measured at average depth x [m] after exposure time t [s] [% by mass of concrete], C_s is the calculated content of ion at the exposed surface [% by mass of concrete], C_i is the initial content of ion [% by mass of concrete], D_{nss} is the non-steady state diffusion coefficient of ion [m^2/s], and $\mathrm{erf}_{(x)}(z)$ is the Gaussian error function [–].

2) Actual chloride transport concept

The error-function $\mathrm{erf}_{(x)}(D_{nss}, C_s, x, t)$ is a mathematical solution to "Fick's 2nd law for :

- $C(x = 0, t) = C_s$
- $C(x, t = 0) = 0$
- $D_{nss} = const.$

Fick's 2nd law is a mass-balance equation, by rearranging Equation (25):

$$\frac{\partial C}{\partial t} = -\frac{\partial}{\partial x}\left(-D \cdot \frac{\partial C}{\partial x}\right) \tag{27}$$

Where the $(-D \cdot \partial C / \partial x)$ is the chloride flux (q_{Cl}). Additionally, a mass-balance must describe the total amount of substance, i.e. the chloride content C in Equation (27) must be the total amount of chloride (C_{tot}).

$$\frac{\partial C_{tot}}{\partial t} = -\frac{\partial}{\partial x} \cdot q_{Cl} \tag{28}$$

Consequently, by comparing equations (27) and (28) it is obvious that the flux of chloride is described by:

$$q_{Cl} = -D \cdot \frac{\partial C_{tot}}{\partial x} \tag{29}$$

The Fick's 2nd law used for chloride ingress into concrete utilizes the total amount of chloride C_{tot} as the flow potential.

3.4 Leaching of Concrete Constituents

3.4.1 Description of the decalcification (leaching) process

The decalcification process is usually described by the dissolution of portlandite and C–S–H in hydrated cement systems exposed to pure water, even though dissolution can be observed in other environments such as seawater. The leaching of ions (mainly calcium and hydroxide) from the pore solution to the external environment is responsible for the dissolution of these hydrates. This phenomenon typically affects structures which have been in contact with pure and acidic waters for long periods: dams, water pipes, radioactive waste disposal facilities, etc. Over the past two decades, it has been identified as a very relevant issue for nuclear waste storage [35]. The consequences of ionic leaching are an increase of the porosity and permeability, and a loss of mechanical strength.

In cement materials, leaching processes involves mainly the transportation of ions from the interior of the material, through its pore system, outwards into the surroundings. In the leaching process, solid compounds in the concrete are dissolved by water that penetrates it and are transported away, either by (i) diffusion based on the concentration gradients, or by (ii) convection through the flow of water. The narrower the flow paths in the concrete, the less the convection flux (Table 1) and the greater the number of ions that flows by diffusion.

Table 1. Relation of pore radius to permeability coefficients [36].

Pore radius (m)	Permeability coefficient (m/s)	Transfer
$< 10^{-7}$	$< 10^{-10}$	Molecular diffusion
$10^{-7} - 10^{-5}$	$10^{-10} - 10^{-9}$	Molecular flow
$> 10^{-5}$	$> 10^{-9}$	Viscous flow

As shown in Figure 15, when cementitious materials are exposed to aggressive solutions, there are three main physicochemical processes for calcium: (i) dissolution of solid-phase calcium in cementitious materials, (ii) diffusion of calcium ions in pore solution, and (iii) reaction with other ions.

Among them, the dissolution of calcium from cement hydrates to the pore solution is regarded as the calcium leaching process. The dissolution of calcium in cement hydrates is controlled by the solubility equilibrium in the C–S–H system.

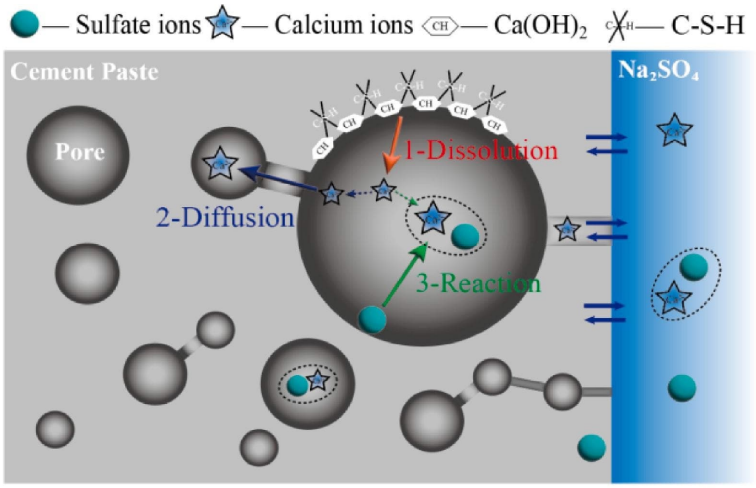

Figure 15. The process of calcium leaching – The diagram of dissolution-diffusion–reaction of calcium [37].

In the post-closure phase, the cement paste can leach out of the concrete. Cement hydrates can be soluble in water. The leached material has very high pH value and provides structural integrity to the concrete. Therefore, with excessive leaching of the cement paste, the pH value of the concrete falls greatly (from around 13 pH to 9-10), and the porosity of the concrete increases, which leads to accelerated damage. Due to the increased porosity, the remaining concrete material is more exposed to other forms of attack (sulfates and chlorides).

The leaching process is dependent on the stability of the pore solution. This stability can be affected when the concrete is submerged underwater, where the concentration gradient between the pore solution and the water solution causes instabilities to the equilibrium. The pore solution originally has a high pH level, and the water solution surrounding the concrete has a much lower pH level. Due to this instability, the dissolution of material from the cement phases can occur to equilibrate the solutions, starting with $Ca(OH)_2$ and aluminates in the concrete matrix, which are more soluble than C-S-H. At a certain point, after the leaching of $Ca(OH)_2$ and the depletion of calcium ions in the concrete matrix, the decalcification and dissolution of calcium in C-S-H occurs, resulting in further pH reductions and loss of calcium.

The leaching of $Ca(OH)_2$ in the cement paste causes many problems to the concrete. $Ca(OH)_2$ typically occupies a sizable volume of concrete, and when it is leached, the porosity and the voids in the concrete matrix increase, resulting in easier deterioration to the structure. The leaching of $Ca(OH)_2$ also reduces the strength properties of concrete. The C-S-H in the concrete matrix can also be leached out when the $Ca(OH)_2$ levels are reduced in the concrete. Groundwater comes into contact with C-S-H from the $Ca(OH)_2$ voids, and that leads to decalcification and leaching in the C-S-H gel in the concrete. The remaining silica gel is much weaker, which in turn means that the strength in the remaining concrete is decreased. The concentration of Ca ions in the water is important in understanding the dissolution behavior of calcium ions. According to [38], the dissolution of $Ca(OH)_2$ from the pore solution in the cement paste starts when the concentration of Ca in the water drops below 22 mmol/L. Dissolution of calcium ions from the C-S-H gel in the pore solution begins when the Ca concentration in the pore solution drops beyond that, with a study stating 1.8 mmol/L as the start of the C-S-H dissolution [39].

The leaching process is time dependent, and it may take hundreds or thousands of years for the C-S-H in the concrete to be depleted. LILW repositories are expected to act as a barrier for very long periods of time, which makes the depletion of $Ca(OH)_2$ and subsequently the leaching of C-S-H a concern.

3.4.2 Modeling the leaching process

The calcium leaching in cement-based materials is a coupled chemical equilibrium/diffusion phenomenon [37].

$$\phi(x,t) \cdot \frac{\partial C(x,t)}{\partial t} = D(x,t) \cdot \frac{\partial^2 C(x,t)}{\partial x^2} \cdot \frac{\partial C_s(x,t)}{\partial t} \quad (30)$$

where $C(x,t)$ is the Ca2+ concentration in the liquid phase, $C_S(x,t)$ is the content of Ca in solid phase, $\phi(x,t)$ is the porosity and $D(x,t)$ is the effective diffusion coefficient of Ca2+ ions.

In Equation (30), the influence of phenomena such as chemical activity, convection and electrical coupling is neglected. The calcium content in solid $C_S(x,t)$ is calculated from its relationship with calcium concentration in solution (Figure 16).

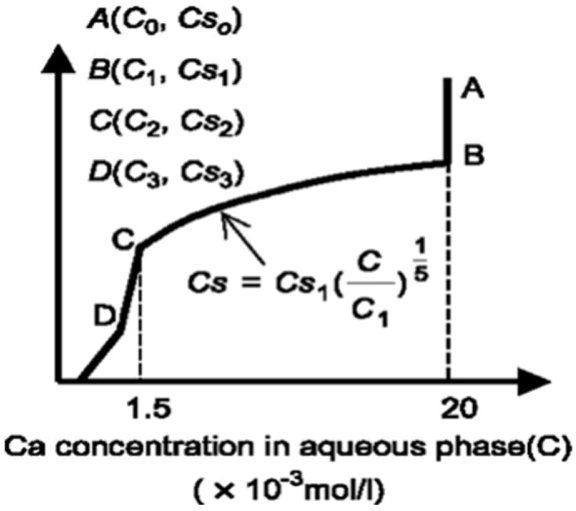

Figure 16. Relationship between Ca concentrations in the solution and the solid [37].

Another approach enables the strong interaction between calcium leaching and the micro-macro solid features of concrete to be consistently taken into account is presented in Figure 17.

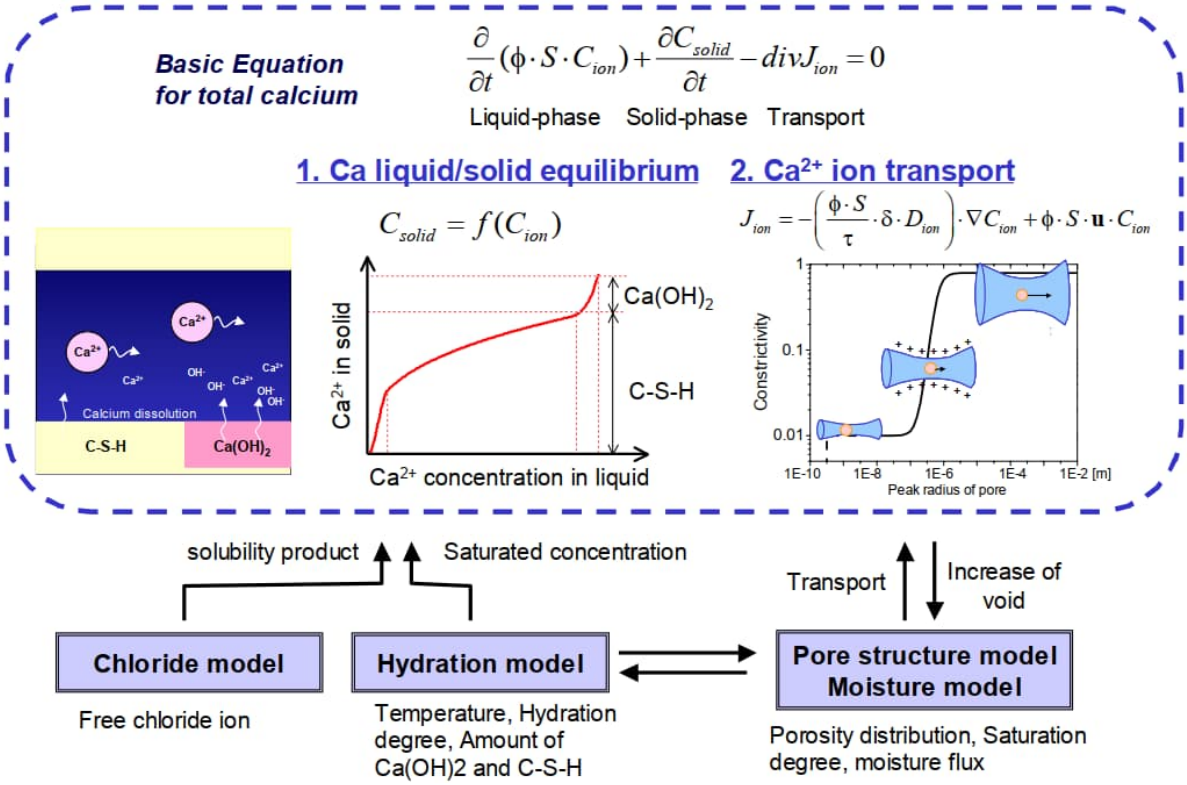

Figure 17. Calcium leaching model coupled with time-dependent material properties [40].

Law of conservation of mass for calcium

Momentum, energy, and material flows must satisfy the conservation laws. As the governing equation for calcium mass conservation, Equation (31) relates the total mass of calcium in the pore solution and the solid phase calcium in the system.

$$\underbrace{\frac{\partial}{\partial t}(\phi \cdot S \cdot C_{ion})}_{Liquid-phase} + \underbrace{\frac{\partial C_{solid}}{\partial t}}_{Solid-phae} - \underbrace{div(J_{ion})}_{Transport} = 0 \quad (31)$$

where, ϕ is porosity [m^3/m^3], S is degree of saturation [-], C_{ion} is the molar concentration of calcium ions in the liquid phase [$mmol/m^3$], C_{solid} is the amount of calcium in the solid phase [$mmol/m^3$], and J_{ion} is the flux of calcium ions [$mmol/m^2 \cdot s$].

The first and second terms of Equation (31) represent the increments in the amount of calcium in the liquid and solid phases per unit time and volume, respectively. The relation between

calcium ion concentrations in the liquid and solid phases is given by the solid-liquid equilibrium model, as described later. Phase transformation (i.e., dissolution from solid to liquid phases or precipitation from liquid to solid phases) is implicitly expressed by assuming a quasi-equilibrated process. The third term of the equation represents the diverging mass flux. The calcium ion flux at a specific boundary surface is expressed by [40]:

$$q_S^{ca} = -h_{ca}\left(C_{ion} - C_{s,ion}\right) \tag{32}$$

where, q_S^{ca} represents the flux of calcium ions into the porous medium at the surface [mmol/m^2-s], h_{Ca} is the surface calcium ion emissivity coefficient [m/s], and $C_{S,ion}$ is the environmental concentration of calcium ions [mmol/l]. The value of the coefficient is assumed to be $1.0 \cdot 10^{-3}$ [m/s].

Solid-liquid equilibrium for calcium

Another mathematical formulation considering the thermodynamic equilibrium of calcium in the solid and liquid phases is presented in Equation (33).

$$C_{solid} = f(C_{ion}) = A \cdot \left\{ C_{C-S-H} \cdot \left(\frac{C_{ion}}{C_{sat}}\right)^{1/3} \right\} + B$$

$$A = \begin{cases} -\frac{2}{x_1^3}(C_{ion})^3 + \frac{3}{x_1^2}(C_{ion})^2 & (0 \le C_{ion} \le x_1) \\ 1 & (x_1 < C_{ion}) \end{cases} \tag{33}$$

$$B = \begin{cases} 0 & (0 \le C_{ion} \le x_1) \\ \frac{C_{CH}}{C_{satu} - x_2} \cdot (C_{ion} - x_2)^3 & (x_1 < C_{ion}) \end{cases}$$

where, C_{C-S-H} is the amount of calcium in the solid phase of the C-S-H gel [mmol/m^3], C_{CH} is the amount of calcium in the solid phase of the calcium hydroxide [mmol/m^3], C_{satu} is the saturated liquid phase calcium ion concentration [mmol/l], x_1 is the liquid phase calcium ion concentration when the rapid transition of C-S-H gel into silica gel begins [mmol/l], and x_2 is the liquid phase calcium ion concentration when the calcium hydroxide has completely dissolved and the dissolution of C-S-H gel begins [mmol/l].

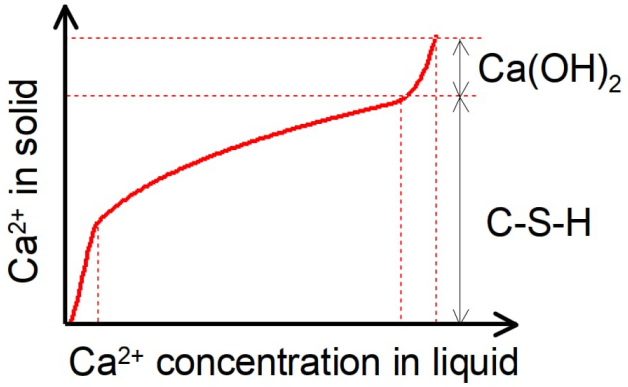

Figure 18. Solid-liquid equilibrium model for calcium.

Transport of calcium ions

By considering both diffusion and advection, the flux of calcium ions transported in a porous media is written as (see Figure 17),

$$J_{ion} = \underbrace{-\left(\frac{\phi \cdot S}{\tau} \cdot \delta \cdot D_{ion}\right) \cdot \nabla C_{ion}}_{Component\ of\ molecular\ diffusion} + \underbrace{\phi \cdot S \cdot u \cdot C_{ion}}_{Advection} \quad (34)$$

where, τ is tortuosity, δ is constrictivity, D_{ion} is the diffusion coefficient of a calcium ion [m2/s], $\nabla^T = [\partial/\partial x, \partial/\partial y, \partial/\partial z]$ is the nabla operator, and $u^T = [u^x, u^y, u^z]$ is the velocity vector of a calcium ion transported by solution flow [m/s]. By treating the capillary and gel pores in the cement paste as ion transport pathways, the porosity, ϕ, is expressed by the following equation:

$$\phi = \phi_{cp} + \phi_{gl} \quad (35)$$

where, $\phi_{cp}\ and\ \phi_{gl}$ are the porosities of capillary and gel pores, respectively. Here, it is assumed that no ion is transported into the interlayer pores of the cement paste since the molecular-related size of the interlayer space is too small to allow substantial room of any ion.

The first term of Equation (34) represents the component of molecular diffusion, while the second is a component representing advection driven by the flow of liquid water in the pore. The velocity of calcium ions related to advection is assumed to reflect the bulk motion of the

condensed water, it is determined from the transport model for the liquid phase [40]. The diffusion coefficient of calcium ions is expressed according to Einstein's theorem by,

$$D_{ion} = R \cdot T \cdot \frac{\lambda_{ion}}{Z_{ion}^2 \cdot F^2} \tag{36}$$

where, R is the ideal gas constant [J/mol-K], λ_{ion} is the molar conductivity of an ion [Sm^2/mol], Z_{ion} is the ion valence (=2), and F is the Faraday constant = 96485.3399 [C/mol].

Regarding the molar conductivity of an ion, λ_{ion}, temperature dependency is taken into account by the Arrhenius law as,

$$\lambda_{ion} = \lambda_{ion\_25} \cdot \exp\left\{-1700\left(\frac{1}{T} - \frac{1}{298}\right)\right\} \tag{37}$$

where, λ_{ion_25} is the molar conductivity of an ion at 25°C, T is the temperature [°C].

Ion transport in a porous media like concrete is affected by the micro pore structure. The effect of pore structure is expressed in terms of porosity, degree of saturation, tortuosity, and constrictivity. Tortuosity is defined as a function of porosity, while constrictivity is a function of pore radius.

Tortuosity expresses the increased length of actual ion transport pathways in accordance with the geometrical connectivity of pore spaces. Tortuosity is thought to be higher for cement paste with finer pores at lower W/C ratios and lower at larger W/C ratios or where coarse pores have been caused by leaching.

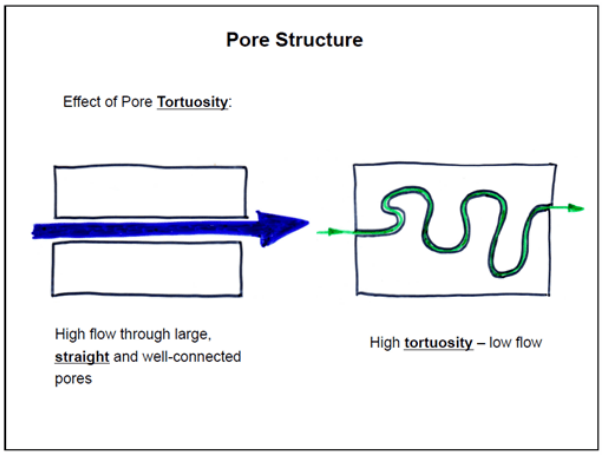

Figure 19. Higher tortuosity due to the presence of aggregates increases the length of the 'path' inside the concrete, reducing the flow of ions [41].

The tortuosity of pores in the cement paste, τ_{paste}, is assumed to be expressed in terms of effective porosity, ϕ_{paste} as presented in Figure 20 [40].

$$\tau_{paste} = -1{,}5\tanh\{8.0(\phi_{paste} - 0.25)\} + 2.5$$
$$\phi_{paste} = \frac{\phi_{cp} + \phi_{gl}}{V_{paste}} \quad (38)$$

where, φ_{paste} is the effective porosity representing the sum of gel and capillary pores effective as ion transport pathways per unit volume of cement paste [m^3/m^3] and V_{paste} is the unit volume ratio of cement paste [m^3/m^3].

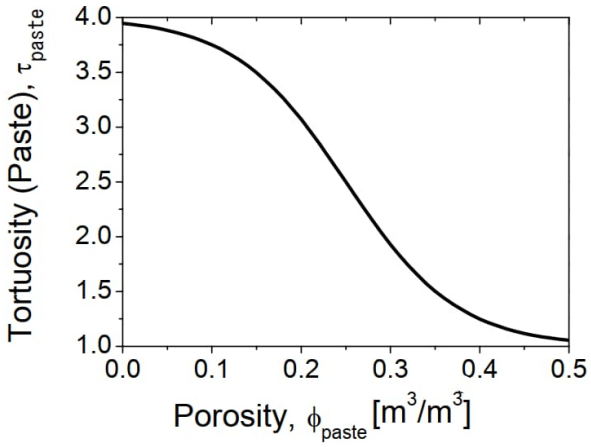

Figure 20. Modeling of tortuosity for cement paste.

Constrictivity is formulated as an expression of the effect of pore size, which is the main determinant of constrictivity. Porosity and pore size distribution were taken into account in one past study of constrictivity. The constrictivity of pores in a cement paste is defined with respect to the peak pore radius by Equation (39) and Figure 21.

$$\delta = 0.395\tanh\{4(\log(r_{cp}^{peak}) + 6.2\} + 0.405$$
$$\delta = 0 \; for \; r_{cp}^{peak} \leq \frac{a_{ca}}{2} \quad (39)$$

where, r_{cp}^{peak} is the peak capillary pore radius [m] and a_{Ca} is an ion diameter parameter for calcium ions = $0.6 \cdot 10^{-9}$ m.

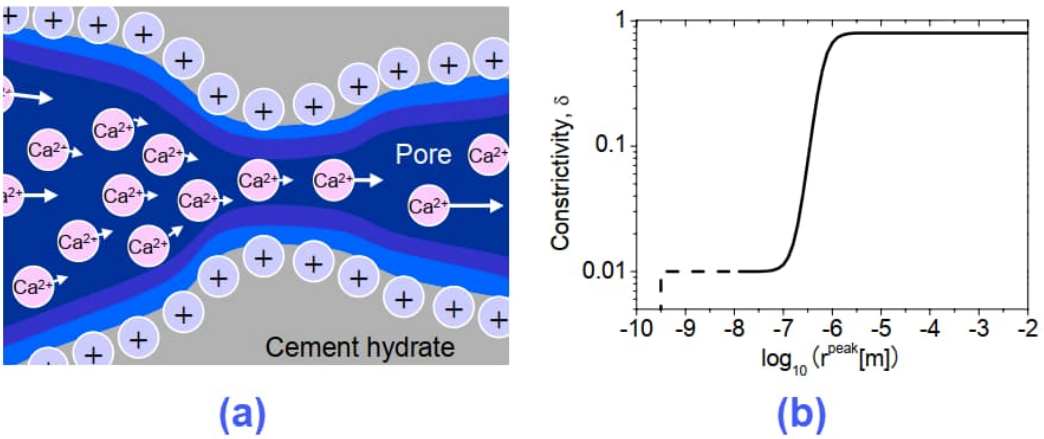

Figure 21. (a) Effect of electrostatic repulsion and (b) Modeling of constrictivity [40].

3.5 Sulfate and thaumasite attacks

Cement-based materials exposed to sulfate-bearing solutions such as some natural or polluted ground waters (external sulfate attack), or by the action of sulfates present in the original mix (internal sulfate attack) can show signs of deterioration. Sulfate ions react with ionic species of the pore solution to precipitate gypsum ($CaSO_4.2H_2O$), ettringite ($[Ca_3Al(OH)_6{\cdot}12H_2O]2{\cdot}(SO_4)_3{\cdot}2H_2O$) or thaumasite ($Ca_3[Si(OH)_6{\cdot}12H_2O]{\cdot}(CO_3){\cdot}SO_4$) or mixtures of these phases. The precipitation of these solid phases can lead to strain within the material, inducing expansion, strength loss, spalling and severe degradation [42].

3.5.1 Description of the sulfate attack process

The existence of excessive sulfate ions inside the concrete can cause damage to the structure. Sulfate ions can react with the mineral phases of the concrete, causing some alteration to the mineral phases. The product of the reaction is ettringite, which can lead to chain reactions that create gypsum and more ettringite. Both the ettringite and gypsum are expansive substances (their volume is larger than the original materials), and that expansion can lead to cracking of the concrete structure.

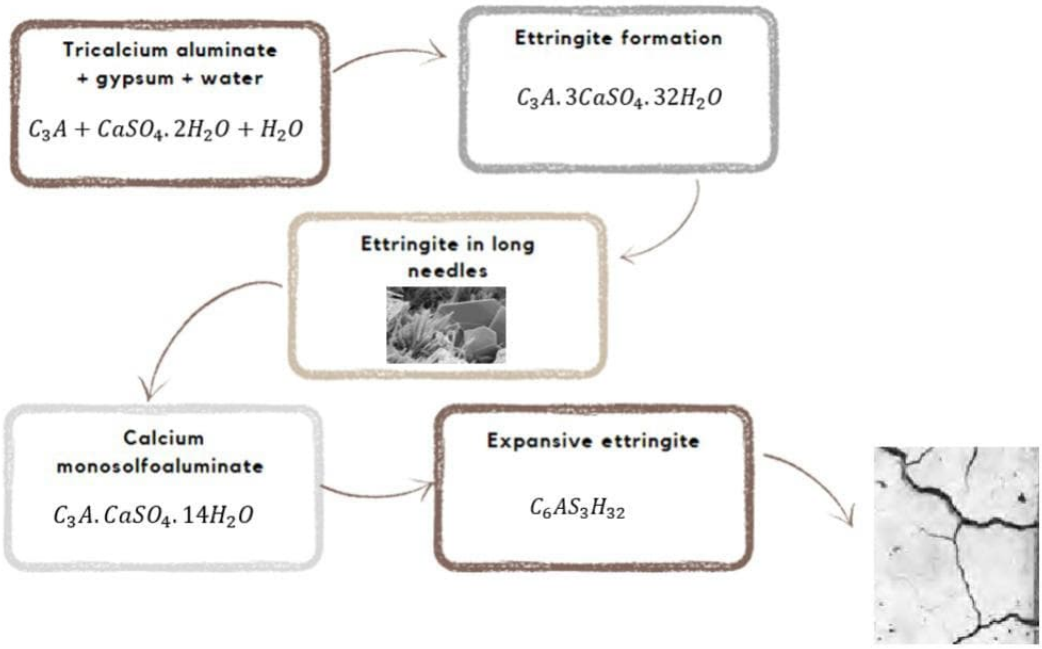

Figure 22. Mechanism of sulfate attack, leading to ettringite formation and concrete damage [43], [44].

Sulfate ions can come from internal and external sources. Sulfates can be present in the concrete through the addition of gypsum in the cement (which is used moderately as a retarder to avoid flash setting of the concrete), or with aggregates. Sulfates can also be present in the concrete's environment (such as soil, seawater, and groundwater), from which it can penetrate through the concrete's microstructure. The presence of a small amount of sulfate ions in the concrete is normal, as it is used as a retarder, and it does not pose any concern. However, when the sulfate content exceeds a certain limit, chemical reactions can occur with some of the mineral phases in the concrete matrix, leading to gypsum and ettringite formation.

The degradation that occurs with sulfate attacks starts when the sulfate ions (from either external or internal sources) react with the portlandite ions in the cement paste in the presence of sufficient moisture, creating gypsum. Gypsum can then react further with the cement phases to produce ettringite needles in the concrete. Both gypsum and ettringite are larger than the original material, leading to internalized stresses in the concrete, which in turn cause internal cracking of the concrete. Ettringite can further react with aluminates in the cement phases to produce monosulfate aluminates (Afm). Figure 23 shows a Scanning Electron Microscopy (SEM) image of a concrete sample that exhibits sulfate attack. Ettringite needles can be seen in the image, as well as some cracks in the concrete that occurred due to the formation of ettringite.

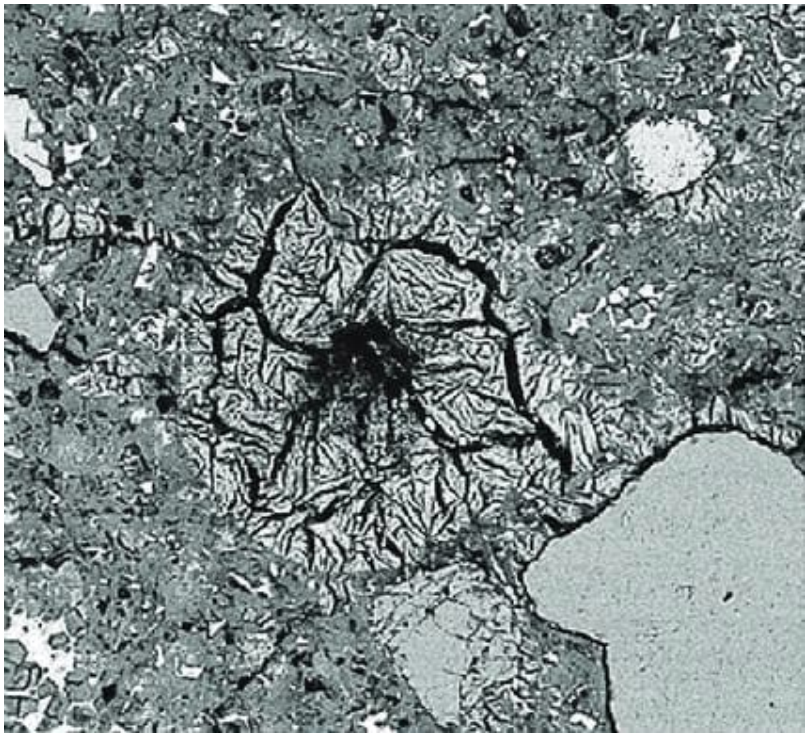

Figure 23: SEM image of ettringite formation in a concrete sample [45].

The formation of ettringite can be shown in the reaction expression in (40) [46], [47]:

$$3C\bar{S}H_2 + C_3A + 26H \rightarrow C_6A\bar{S}_3H_{32}$$

$$3C\bar{S}H_2 + C_3AH_{13} + 14H \rightarrow C_6A\bar{S}_3H_{32} + CH \quad (40)$$

$$2C\bar{S}H_2 + C_4A\bar{S}H_{12} + 16H \rightarrow C_6A\bar{S}_3H_{32}$$

These reactions can be lumped into expression (41):

$$q.C\bar{S}H_2 + CA \rightarrow C_6A\bar{S}_3H_{32} \quad (41)$$

Where q is the weight coefficient of gypsum in the reactions, expressed as $q = 3\mu_1 + 3\mu_2 + 2\mu_3$, and μ represents the aluminate (gypsum) content in the reaction.

Sulfates can migrate to the concrete's microstructure with other ions, such as calcium sulfates and magnesium sulfate. The specific form of sulfate ions present in the concrete's environment can affect the form and extent of damage that the concrete exhibits. The main parameter is the solubility of the ion. For example, magnesium sulfates are more soluble in water, and this solubility can increase the rate of damage. Magnesium can also interact with

other cement phases, leading to more thorough deterioration. Magnesium reactions in the cement phases lead to the formation of Brucite, $Mg(OH)_2$, or react with the C-S-H phases in cement to produce magnesium silicate hydrates, M-S-H [48]. The formation of both Brucite and M-S-H is not favorable, as they result in the depletion of calcium in the concrete and produce weaker and incohesive phases.

Thaumasite Sulfate Attack (TSA) is a special form of sulfate related damage. TSA is not very common in conventional structures, and it requires certain conditions to commence. A study found that specific temperatures (around 5 degrees Celsius is preferable, but it can occur at 10-15 degree as well) and the presence of moisture are needed. A Swiss study also found that thaumasite can form in concrete structures even in temperatures over 20 degrees Celsius [49]. The damage that occurs to the concrete's microstructure due to TSA is much more severe than the typical sulfate attacks, as it attacks C-S-H of the cement paste, instead of attacking $Ca(OH)_2$. This change in the cement phase leads to loss of strength of the material. The TSA seems to form mush-like material from the concrete phases, which surround the aggregate. This thaumasite mush is soft compared to the original material, indicating severe alteration to the concrete. Figure 24 shows a concrete specimen that is deteriorated with TSA.

Figure 24: Concrete samples showing thaumasite formation [50].

Thaumasite in concrete comes in the form of $CaSiO_3CaSO_4CaCO_315H_2O$, or the shortened form $C_3S\bar{S}\bar{C}H_{15}$. The thaumasite reaction requires the presence of sulfate and carbonates in the concrete, or in the concrete environment. Carbonates are also necessary for thaumasite

formation, which can come from the mix constituents, or from atmospheric CO_2, which can carbonate the cement phases [51], [52].

TSA in the concrete matrix can initiate when the sulfate attacks the concrete, creating gypsum and ettringite, as well as changing the cement phases in the concrete. TSA also requires the presence of carbonates in the concrete matrix, which can be present in the cement phases, and can also be present due to carbonation of the concrete. When the TSA is initiated (in the presence of moisture), the C-S-H in the cement paste is attacked directly, with the reaction product being soft and mushy, which makes TSA much more severe than conventional sulfate attacks. The rate of TSA can be slow at the start, but the reaction becomes rapid when more thaumasite is formed in the material.

Sulfates ions required for the TSA can come from external sources, such as soil and groundwater. In repository conditions during the post-closure phase, the surrounding groundwater becomes the source of sulfates for the TSA reaction, and it will also provide the moisture requirements for the TSA reaction to occur. The conditions in waste repositories during the post-closure period can be somewhat favorable for TSA, especially when considering the given timescale, which allows lime leaching and traditional sulfate attacks to occur as well increasing the risk of thaumasite formation. This requires additional care and precautions to avoid possible severe concrete degradation due to thaumasite damage. A common approach to prevent potential sulfate attack is to improve the chemical resistance of the concrete.

3.5.2 External sulfate attack modeling

Empirical, mechanistic, and numerical models are proposed in literature for predicting the behavior of cement systems exposed to sulfate-laden environments.

- Empirical models estimate the sulfate resistance factor, the expansion under sulfate attack or the location of the visible degradation zone.
- Mechanistic models typically attempt to take into account the mechanisms leading to the deterioration of the material.

These models usually predict the rate of sulfate attack and the fractional or volumetric expansion. Ionic transport models simulate the chemical reactions occurring during sulfate attack and, in some cases, also estimate the damage caused by expansion.

Sulfate reacts more strongly with cement substances and models need therefore to include mineralogical transformations. The complexity of the problem is increased by the fact that concrete structures in contact with a sulfate-bearing solution can not only be subjected to sulfate attack but are also usually affected by decalcification. The chemical reactions occurring under sulfate attack can be summarized by the solubility constants of ettringite, monosulfate and gypsum given in Table 2 [53].

The solubility product constant (is the equilibrium constant for a solid substance dissolving in an aqueous solution. It represents the level at which a solute dissolve in a solution. The more soluble a substance is, the higher the K_{sp} value it has. Consider the general dissolution reaction below (in aqueous solutions):

$$aA(s) \rightleftharpoons cC(aq) + dD(aq) \tag{42}$$

To solve for the K_{sp} it is necessary to take the molarities or concentrations of the products ($cC\ and\ dD$) and multiply them. If there are coefficients in front of any of the products, it is necessary to raise the product to that coefficient power (and also multiply the concentration by that coefficient). This is shown below:

$$K_{sp} = [C]^c[D]^d \tag{43}$$

Note that the reactant, aA, is not included in the K_{sp} equation. Solids are not included when calculating equilibrium constant expressions, because their concentrations only has an insignificant effect on the outcome, and therefore they are omitted. Hence, K_{sp} represents the maximum extent that a solid that can dissolve in solution.

Table 2. Solubility constants of solid phases involved during sulfate ingress in hydrated cement systems [53].

Name	Chemical Formula	Expression for Equilibrium $(\boldsymbol{K_{sp}})$	$-\boldsymbol{log\ K_{sp}}$
Ettringite	$3CaO.Al_2O_3.3CaSO_4.32H_2O$	$[Ca^{2+}]^6\ [OH^-]^4\ [SO_4^{2-}]^3\ [Al(OH)_4^-]^2$	44.0
Monosulfate	$3CaO.Al_2O_3.CaSO_4.12H_2O$	$[Ca^{2+}]^4\ [OH^-]^4\ [SO_4^{2-}]^1\ [Al(OH)_4^-]^2$	29.4
Gypsum	$CaSO_4.2H_2O$	$[Ca^{2+}]^1\ [SO_4^{2-}]^1$	4.6

3.6 Alkali Aggregate Reaction (AAR)

Alkali Aggregate Reactions (AAR) is a degradation mechanism that can occur to the concrete in the presence of degrading agents in the aggregate. Alkali Silica Reaction (ASR) is the most common form of AAR in concrete structures. ASR occurs when reactive silica in the aggregates reacts with alkalis in the concrete, resulting in the production of an expansive gel (ASR gel) that causes cracks in the concrete matrix due to the expansion, which weakens the concrete and makes it more susceptible to further damage by other degrading mechanisms [54].

ASR can occur in the concrete when free alkalis, which are present from cementitious materials, react with amorphous silica that comes with some types of aggregates. The used aggregates in the concrete are the main driving factor in ASR. The choice of the used aggregates and their origin is therefore important because some natural aggregates are known to contain high amounts of reactive silica that can lead to ASR in the concrete and subsequent damage Due to the reaction. In the Nordic region, and especially in Finland, ASR was usually identified incorrectly as a different form of concrete damage (such as freezing and thawing, because the pattern of ASR and frost damage appears to be similar, and that it was believed that the aggregates used in the region do not cause ASR) before further investigation proved that ASR is indeed the reason for these reactions [55], [56].

There are three required conditions for ASR to occur in the concrete. The concrete must have i) reactive silica, which comes mainly with aggregates, ii) high alkali content, which is associated with the cement and iii) sufficient moisture. Without any of those three conditions, the reaction does not occur, and the concrete is safe from ASR.

When the three conditions are met, ASR can happen in the concrete matrix. The free alkalis can react with amorphous silica that comes from the aggregates. The result from the reactions is alkali silica gel, which is hydrophilic. The gel is located around and through aggregates cracks, which can be shown in the schematic diagram in Figure 25. The hydrophilic nature of the gel causes it to expand with the attracted moisture, leading to map cracks in the structure, as well as discoloration from the excess gel. An example of concrete damaged due to ASR is shown in Figure 26. ASR can be somewhat difficult to study in natural conditons, as it may take over 10 years for the reaction to occur [57]. Laboratory investigation of ASR is possible using accelerated methods, such as the Concrete Prism Test.

Figure 25: Schematic diagram of ASR attack [58].

Another form of AAR is Alkali Carbonate Reaction (ACR). The damage exhibited by the concrete due to this form of attack is very similar to ASR damage. The reaction is not as common as ASR though, because the aggregates that are responsible for the ACR reaction are not used widely as the aggregates associated with ASR.

Figure 26: ASR in a concrete structure, with visible map cracking and leaking gel on the surface.

The occurrence of AAR in LILW repositories is possible, especially in the post-closure phase, where the concrete is submerged and sufficient moisture for the reaction is always present. The choice of both the cement and most importantly the aggregates used in the mixture is important to avoid the occurrence of ASR and damage to the concrete structure. Because the use of suitable materials and aggregates to avoid AAR is possible, it is not explained in detail in this report.

3.7 Combined interaction of degradation phenomena

The interaction between different concrete degradation phenomena is important, as it influences the degradation rate of the structure. An example of that is the interaction between chlorides and sulfates, which becomes even more complex when considering chloride binding and Friedel's salt. The sulfate ions interact with the aluminate phases in the cement paste, which results in the creation of ettringite. Friedel's salt forms when chlorides interact with aluminates as well. The formation of either ettringite or Friedel's salt can lead to the blockage of pores in the concrete, slowing the ingress of chemicals into the concrete. Chlorides and sulfates are also competing for aluminates in the concrete phases, which can affect the rate of degradation in the concrete.

As discussed in the previous chapters, the porosity of the concrete changes with degradation, which could slow down the degradation rate at first due to pore blockage. After a certain threshold, however, the porosity increases due to cracks of the concrete, which can accelerate the rate of further degradation phenomena. These inter-related changes are not always studied, as they can sometimes be overlooked in research focusing on one specific reaction in the concrete.

Considering complex and interconnected effects that lead to changes in the concrete in simulations can improve the conceptual models. An example of using different parameters in degradation modelling was shown in a recent study [46], where the combined effect of chloride ingress, sulfate attack, and leaching were modelled. The porosity changes that occur with time due to the different phenomena were considered in a system of equations (pore blockage by Friedel's salt, or porosity increase due to leaching, for example), which is shown in equation (44):

$$\frac{\Delta V}{V} = \underbrace{\left(\frac{\Delta V}{V}\right)_{R}}_{Changes,chemical\ reaction} - \underbrace{\left(\frac{\Delta V}{V}\right)_{Leach}}_{Changes,leaching} \quad (44)$$

The terms on equation (44) reflect the changes in volume (due to consumption of aluminates or formation of Friedel's salt, for example), which are used in the model to update the

porosity, considering the intricate kinetics between the interacting agents. Another study on a numerical model [59] for concrete that is subjected to both leaching and sulfate attack found that establishing the relationship between the calcium leaching and sulfate-based expansion of the concrete is necessary, as ignoring the effects of calcium leaching as a whole would present a decrease in the estimated expansion due to external sulfates, and it would overestimate the expansion changes if the model did not consider the porosity changes due to calcium leaching. The porosity changes lead to an increase in the porosity of the concrete, giving the expansive product of sulfate reaction more room before causing internalized stresses in the concrete.

3.8 Shortcomings

A few problems typically arise from using computational numerical models to predict the long-term degradation behavior of concrete structures. The main problem can be summarized in the simplification nature of computational models, which can result in an incorrect representation of the results. This can be seen in the simple form of Fick's law for the determination of chloride diffusion coefficient, due to the simplifications made to obtain the equation, the analytical solution is not representative of most scenarios. The equation is also widely used, incorrectly, to calculate the so-called apparent diffusion coefficient, for cases that do not fit the simplified model. The lack of understanding of the procedure of obtaining the numerical equation can lead to these sorts of problems.

The obtained models in concrete studies are typically not suitable for all cases, as they are most of the time dedicated to a specific scenario, which can result in errors when those models are applied to a general case that is outside the framework of the model. As mentioned in the previous examples, some developed models are made for specific exposure conditions (complete saturation, for example), or for the addition of specific SCMs in the concrete mix, and so on. This reinforces the need to understand these numerical approaches.

3.9 Opportunities and possible improvements for concrete degradation models

An opportunity for concrete degradation models arises with the development of Machine Learning (ML) algorithms and Artificial Intelligence (AI), which can be used in the analysis of degradation patterns in reinforced concrete to understand and determine the characteristics

of degradation, and the life expectancy of the structure based on the specific input parameters of the structure. AI tools can offer a different outlook on the studies, as their numerical capabilities are not limited by comprehension and judgement.

AI methods can be used in the analysis of concrete degradation, to assess and predict future degradation based on the known data. These methods can be used to observe complex patterns, which can be useful in determining future material behavior. The complex nature of ionic interactions in the cement mixture makes the use of ML tools beneficial, and those algorithms can utilize additional results to reinforce the model and improve its accuracy.

In 2021, a study by Prakash et al. [60] was made to investigate and review degradation models in concrete. The study is made to for the assessment of infrastructure life expectancy. The reviewed models were classified into different categories based on their principles, whether they are based on physics, statistics, and so on. This sort of framework can be applied for specific degradation phenomena, opposed to a wide life expectancy approach, to analyze concrete degradation in various exposure environments.

Another study [61] was conducted using an Artificial Neural Network (ANN) to predict the chloride diffusivity in reinforced concrete. The developed ANN model utilized 13 different parameters (concrete mix, SCMs, exposure time, exposure environment, etc.). The results showed a strong correlation between the values obtained by the model and the experimental results.

4. Summary and conclusions

In Finland, the use of clean energy and nuclear power is prominent. This use can pose some challenges when it comes to the long-term disposal of radioactive waste, which does not come without hazards. The use of engineered barrier systems is therefore necessary, especially in the final disposal of nuclear waste. Reinforced concrete materials are important in the engineered barrier systems, due to their contribution to waste containment. The current waste disposal facilities in Finland in both Olkiluoto and Loviisa are in use, and with planned expansions. The intermediate level wastes are enclosed by concrete, and the these waste caverns will be backfilled when the operation period of the repositories ends. Studies on the degradation of concrete in repository settings are therefore important to understand the potential deterioration that could occur to reinforced concrete during its functional life.

Concrete degradation is quite complex. Ionic interactions and changes occurring to the concrete structure are influenced by the degrading agents present in the concrete and its environment, as well as the changes themselves. The different phenomena that cause concrete degradation have an influence on one another, which makes studying the degradation cases challenging. This becomes even more difficult in long-term studies, where the age of the structure exceeds the human experience with modern cement concrete, such as the radioactive waste repositories. Therefore, an assessment and analysis of the degradation of concrete is needed to develop the experience and knowledge of the deterioration of reinforced concrete structures.

In waste repository settings, concrete is subjected to various deterioration mechanisms that affect its performance during its lifespan. Deterioration is mainly driven by groundwater flow. The duration of different mechanisms, as well as their starting time and rate of effect differs based on the groundwater flow, the concrete mix, the composition of groundwater, and so on. Concrete structures in LILW repositories must stay intact for very long lifespans, which can be upwards of thousands of years. This large timescale is beyond the capacity of traditional physical studies, which encourages the development and use of adequate computational tools in studies and analysis of reinforced concrete. Modelling tools and methods are constantly developed, to further enhance the conceptual model framework and improve the reliability of long-term concrete research. These new tools and methods are reviewed during the PERCO2 research project.

In reinforced concrete degradation model, the detail of the model can vary (structure, element, or even microstructure scale). The parameters of the model, as well as the interaction kinetics are also different. In a lot of studies, the used model is limited due to computation restraints. The models might also be suitable for a specific scenario. Models can

also be used inadequately in some instances. Therefore, it is important to understand the features and uses of the applied or developed model, to ensure that it supports the studied case.

Concrete studies have evolved recently. Modelling has become a powerful tool for analysis and degradation prediction. More complex and dynamic interactions of different agents are being considered in the development of some models, which are suitable for long-term studies for concrete subjected to several different degradation mechanisms. Further development of the model framework is encouraged to have an accurate depiction of the degradation phenomena. The use of AI tools can also be beneficial in long-term degradation studies, as they can give a different perspective of the transport interaction and degradation behavior of reinforced concrete in repository setting.

References

[1] Teollisuuden Voima Oyj (TVO), “TVO - Operational waste.” Accessed: Aug. 21, 2023. [Online]. Available: https://www.tvo.fi/en/index/production/nuclearwastemanagement/operationalwaste.html

[2] Fortum, “Nuclear waste management.” Accessed: Aug. 21, 2023. [Online]. Available: https://www.fortum.com/energy-production/nuclear-power/nuclear-waste-management?vtab=accordion-item-28736

[3] J. Koťátková, J. Zatloukal, P. Reiterman, and K. Kolář, “Concrete and cement composites used for radioactive waste deposition,” *J Environ Radioact*, vol. 178–179, pp. 147–155, Nov. 2017, doi: 10.1016/J.JENVRAD.2017.08.012.

[4] E. Vesikari and P. Koskinen, “Durability of Concrete Barriers in Final Depositories of Nuclear Waste,” Espoo, Feb. 2012. Accessed: Aug. 27, 2023. [Online]. Available: http://kyt2014.vtt.fi/julkaisut/koskinen_et_vesikari_VTT_R_01185_12.pdf

[5] M. Garamszeghy, “Disposal of Low-and Intermediate-Level Waste: International experience,” Feb. 2018. Accessed: Aug. 23, 2023. [Online]. Available: https://radwasteplanning.ca/sites/default/files/lilw_white_paper_final.pdf

[6] Stuk, “Radiation and Nuclear Safety Authority Joint Convention on the Safety of Spent Fuel Management and on the Safety of Radioactive Waste Management,” Oct. 2017, Accessed: Aug. 23, 2023. [Online]. Available: https://www.iaea.org/sites/default/files/national_report_of_finland_for_the_6th_review_meeting_-_english.pdf

[7] I. A. E. AGENCY, “Status and Trends in Spent Fuel and Radioactive Waste Management,” *Status and Trends in Spent Fuel and Radioactive Waste Management*, pp. 1–57, 2018, Accessed: Aug. 23, 2023. [Online]. Available: https://www.iaea.org/publications/11173/status-and-trends-in-spent-fuel-and-radioactive-waste-management

[8] F. Al-Neshawy, A. Ba Ragaa, and J. Punkki, “Comprehensive state-of-the-art report for long-term behaviour of concrete structures in repository environment,” 2022. [Online]. Available: https://aaltodoc2.org.aalto.fi/handle/123456789/119823

[9] M. Otieno, M. Alexander, and H. Beushausen, “Transport mechanisms in concrete – Corrosion of steel in concrete (Initiation, propagation and factors affecting),” Cape Town, South Africa., 2010. Accessed: Nov. 15, 2023. [Online]. Available:

https://ebe.uct.ac.za/sites/default/files/content_migration/ebe_uct_ac_za/848/files/Transport_mechanisms_Corrosion_of_steel_and_Corrosion_Assessment_in_Concrete_-_CSIRG_2010_FINAL_0.pdf

[10] P. A. Claisse, "The transport properties of concrete and the equations that describe them," *Transport Properties of Concrete*, pp. 1–16, 2014, doi: 10.1533/9781782423195.1.

[11] L. Bertolini, B. Elsener, P. Pedeferri, and R. B. Polser, "Transport Processes in Concrete," in *Corrosion of Steel in Concrete: Prevention, Diagnosis, Repair*, Wiley VCH, 2004, pp. 21–48.

[12] C. Gehlen, S. Von Greve-Dierfeld, and K. Osterminsk, "Modelling of ageing and corrosion processes in reinforced concrete structures," *Non-Destructive Evaluation of Reinforced Concrete Structures: Deterioration Processes and Standard Test Methods*, pp. 57–81, Jan. 2010, doi: 10.1533/9781845699536.1.57.

[13] P. A. M. Basheer, S. E. Chidiac, and A. E. Long, "Predictive models for deterioration of concrete structures," *Constr Build Mater*, vol. 10, no. 1, pp. 27–37, Feb. 1996, doi: 10.1016/0950-0618(95)00092-5.

[14] L. Czarnecki and P. Woyciechowski, "Prediction of the reinforced concrete structure durability under the risk of carbonation and chloride aggression," *Bulletin of the Polish Academy of Sciences: Technical Sciences*, vol. 61, no. 1, pp. 173–181, Mar. 2013, doi: 10.2478/BPASTS-2013-0016.

[15] M. Elsalamawy, A. R. Mohamed, and E. M. Kamal, "The role of relative humidity and cement type on carbonation resistance of concrete," *Alexandria Engineering Journal*, vol. 58, no. 4, pp. 1257–1264, Dec. 2019, doi: 10.1016/J.AEJ.2019.10.008.

[16] K. T. Kunal Tongaria, S. M. S.Mandal, and D. M. Devendra Mohan, "A Review on Carbonation of Concrete and Its Prediction Modelling," *Journal of Environmental Nanotechnology*, vol. 7, no. 4, pp. 75–90, 2018, doi: 10.13074/JENT.2018.12.184325.

[17] Hielscher Ultrasonics, "Ultrasound-Enhanced Mineral Carbonation." Accessed: Nov. 14, 2023. [Online]. Available: https://www.hielscher.com/ultrasound-enhanced-mineral-carbonation.htm

[18] J. P. Balayssac, C. H. Détriché, and J. Grandet, "Effects of curing upon carbonation of concrete," *Constr Build Mater*, vol. 9, no. 2, pp. 91–95, Apr. 1995, doi: 10.1016/0950-0618(95)00001-V.

[19] L. Czarnecki and P. Woyciechowski, “Modelling of concrete carbonation; is it a process unlimited in time and restricted in space?,” *Bulletin of the Polish Academy of Sciences. Technical Sciences*, vol. 63, no. 1, pp. 43–54, 2015, doi: 10.1515/BPASTS-2015-0006.

[20] F. Al-Neshawy, “Computerised prediction of the deterioration of concrete building facades caused by moisture and changes in temperature,” Aalto University, Espoo, 2013. Accessed: Sep. 08, 2022. [Online]. Available: http://urn.fi/URN:ISBN:978-952-60-5203-8

[21] V. G. Papadakis, “ESTIMATION OF CONCRETE SERVICE LIFE – The Theoretical Background,” Patras, Greece., 2005. Accessed: Nov. 14, 2023. [Online]. Available: http://users.csa.upatras.gr/~vgpapa/files/book2.pdf

[22] Duracrete, *DuraCrete: Probabilistic Performance based Durability Design of Concrete Structures - Final Technical Report: General guidelines for durability design and redesign*. 2000.

[23] DuraCrete, “General Guidelines for Durability Design and Redesign,” *The European Union-Brite Euram III, Project No. BE95-1347, Probabilistic Performance -based Durability Design of Concrete Structures*, 2000.

[24] O.-P. Kari, “Modelling the durability of concrete for nuclear waste disposal facilities,” Aalto University, Espoo, Finland, 2009. Accessed: Nov. 14, 2023. [Online]. Available: https://aaltodoc.aalto.fi:443/handle/123456789/106682

[25] O. P. Kari and J. Puttonen, “Simulation of concrete deterioration in Finnish rock cavern conditions for final disposal of nuclear waste,” *Ann Nucl Energy*, vol. 72, pp. 20–30, Oct. 2014, doi: 10.1016/J.ANUCENE.2014.04.035.

[26] O.-P. Kari, “Long-term ageing of concrete structures in Finnish rock caverns as application facilities for low- and intermediate-level nuclear waste,” 2015, Accessed: Aug. 23, 2023. [Online]. Available: https://research.aalto.fi/en/publications/long-term-ageing-of-concrete-structures-in-finnish-rock-caverns-a

[27] O.-P. Kari, “Long-term ageing of concrete structures in Finnish rock caverns as application facilities for low- and intermediate-level nuclear waste ,” Concrete magazine (Betonilehti). Accessed: Apr. 08, 2022. [Online]. Available: https://betoni.com/wp-content/uploads/2015/10/BET1503_63-65.pdf

[28] O.-P. Kari, J. Puttonen, V. Hiltunen, and P. Varpasuo, “The Current Status of Modelling of the Ageing of Concrete for Low- and Medium Level Nuclear Waste Storage Facilitie,” in *Proceedings of OECD NEA CSNI workshop on “Concrete ageing in nuclear power plant*

structures", Prague 2008, Prague, May 2002. Accessed: Jun. 13, 2022. [Online]. Available: http://www.kolumbus.fi/pentti.varpasuo/OECD_NEA_wrkshp_Prague_0108Oct_Paper.htm

[29] S. R. Charlton and D. L. Parkhurst, "Modules based on the geochemical model PHREEQC for use in scripting and programming languages," *Comput Geosci*, vol. 37, no. 10, pp. 1653–1663, Oct. 2011, doi: 10.1016/j.cageo.2011.02.005.

[30] U. M. Angst, ; O Burkan Isgor, C. M. Hansson, A. Sagüés, ; Mette, and R. Geiker, "Beyond the chloride threshold concept for predicting corrosion of steel in concrete", doi: 10.1063/5.0076320.

[31] M. Maes and N. De Belie, "Resistance of concrete and mortar against combined attack of chloride and sodium sulphate," 2014, doi: 10.1016/j.cemconcomp.2014.06.013.

[32] A. Abdalkader, "Thaumasite Sulfate Attack in Cement Mortars Exposed to Sulfate and Chloride and Implications to Rebar Corrosion," Faculty of Engineering of the University of Sheffield, Sheffield, UK, 2014. Accessed: Dec. 08, 2023. [Online]. Available: https://core.ac.uk/download/pdf/29030036.pdf

[33] L.-O. Nilsson, "CONCEPTS IN CHLORIDE INGRESS MODELLING," 2003. Accessed: Nov. 14, 2023. [Online]. Available: https://www.rilem.net/images/publis/pro038-003.pdf

[34] G. Rong, T. He, G. Zhang, Y. Li, Y. Wang, and W. Xie, "A review on chloride transport model and research method in concrete," *Mater Res Express*, vol. 10, no. 4, p. 042002, Apr. 2023, doi: 10.1088/2053-1591/ACCB2A.

[35] S. Goñi, M. Frías, R. V. De La Villa, and I. Vegas, "Decalcification of activated paper sludge – Fly ash-Portland cement blended pastes in pure water," *Cem Concr Compos*, vol. 40, pp. 1–6, Jul. 2013, doi: 10.1016/J.CEMCONCOMP.2013.04.002.

[36] T. Ekström, "Leaching of concrete : The leaching process and its effects," LTH, Lund University., Lund, Sweden, 2003. Accessed: Nov. 16, 2023. [Online]. Available: www.byggnadsmaterial.lth.se

[37] D. Zou *et al.*, "Calcium leaching from cement hydrates exposed to sodium sulfate solutions," *Constr Build Mater*, vol. 351, p. 128975, Oct. 2022, doi: 10.1016/J.CONBUILDMAT.2022.128975.

[38] J. Duchesne and A. Bertron, “Leaching of cementitious materials by pure water and strong acids (HCl and HNO3),” *RILEM State-of-the-Art Reports*, vol. 10, pp. 91–112, 2013, doi: 10.1007/978-94-007-5413-3_4/TABLES/3.

[39] P. Faucon, F. Adenot, J. F. Jacquinot, J. C. Petit, R. Cabrillac, and M. Jorda, “Long-term behaviour of cement pastes used for nuclear waste disposal: review of physico-chemical mechanisms of water degradation,” *Cem Concr Res*, vol. 28, no. 6, pp. 847–857, Jun. 1998, doi: 10.1016/S0008-8846(98)00053-2.

[40] K. Nakarai, T. Ishida, and K. Maekawa, “Modeling of Calcium Leaching from Cement Hydrates Coupled with Micro-Pore Formation,” *Journal of Advanced Concrete Technology*, vol. 4, no. 3, pp. 395–407, 2006.

[41] J. Texeira, “Why Measure Concrete Resistivity? .” Accessed: Nov. 20, 2023. [Online]. Available: https://www.giatecscientific.com/education/why-measure-concrete-resistivity/

[42] F. P. Glasser, J. Marchand, and E. Samson, “Durability of concrete — Degradation phenomena involving detrimental chemical reactions,” *Cem Concr Res*, vol. 38, no. 2, pp. 226–246, Feb. 2008, doi: 10.1016/J.CEMCONRES.2007.09.015.

[43] A. Ba Ragaa, “Long-term durability testing of concrete in low and intermediate level waste repositories,” Master’s Thesis, Aalto University, 2023.

[44] O. A. Hodhod and G. Salama, “Developing an ANN model to simulate ASTM C1012-95 test considering different cement types and different pozzolanic additives,” *HBRC Journal*, vol. 9, no. 1, pp. 1–14, 2013, doi: 10.1016/j.hbrcj.2013.02.003.

[45] I. Fernandes, M. A. T. M. Broekmans, and F. Noronha, “Petrography and geochemical analysis for the forensic assessment of concrete damage,” *Criminal and Environmental Soil Forensics*, pp. 163–180, 2009, doi: 10.1007/978-1-4020-9204-6_11/COVER.

[46] P. Wang, R. Mo, X. Zhou, J. Xu, Z. Jin, and T. Zhao, “A chemo-thermo-damage-transport model for concrete subjected to combined chloride-sulfate attack considering the effect of calcium leaching,” *Constr Build Mater*, vol. 306, Nov. 2021, doi: 10.1016/j.conbuildmat.2021.124918.

[47] X. Chen, X. Gu, X. Xia, X. Li, and Q. Zhang, “A chemical-transport-mechanics numerical model for concrete under sulfate attack,” *Materials*, vol. 14, no. 24, Dec. 2021, doi: 10.3390/ma14247710.

[48] T. Zhang, L. J. Vandeperre, and C. R. Cheeseman, "Formation of magnesium silicate hydrate (M-S-H) cement pastes using sodium hexametaphosphate," *Cem Concr Res*, vol. 65, pp. 8–14, Nov. 2014, doi: 10.1016/J.CEMCONRES.2014.07.001.

[49] M. Romer, L. Holzer, and M. Pfiffner, "Swiss tunnel structures: concrete damage by formation of thaumasite," *Cem Concr Compos*, vol. 25, no. 8, pp. 1111–1117, Dec. 2003, doi: 10.1016/S0958-9465(03)00141-0.

[50] M. M. Rahman and M. T. Bassuoni, "Thaumasite sulfate attack on concrete: Mechanisms, influential factors and mitigation," *Constr Build Mater*, vol. 73, pp. 652–662, Dec. 2014, doi: 10.1016/J.CONBUILDMAT.2014.09.034.

[51] : Ashraf, H. M. Abdalkader, C. Lynsdale, and J. Cripps, "Thaumasite Sulfate Attack in Cement Mortars Exposed to Sulfate and Chloride and Implications to Rebar Corrosion," 2014.

[52] C. Shi, D. Wang, and A. Behnood, "Review of Thaumasite Sulfate Attack on Cement Mortar and Concrete," *Journal of Materials in Civil Engineering*, vol. 24, no. 12, pp. 1450–1460, Dec. 2012, doi: 10.1061/(ASCE)MT.1943-5533.0000530/ASSET/86AB159F-2A0D-43A9-8A0F-F73FF852FBC8/ASSETS/IMAGES/LARGE/FIGURE4.JPG.

[53] C. A. Langton and D. S. Kosson, "Chemical degradation review – cementitious barriers partnership," Washington, DC, 2009. Accessed: Nov. 16, 2023. [Online]. Available: https://www-pub.iaea.org/MTCD/Publications/PDF/TE-1701_add-CD/PDF/USA%20Attachment%2005.pdf

[54] R. Esposito and M. A. N. Hendriks, "Literature review of modelling approaches for ASR in concrete: a new perspective," *European Journal of Environmental and Civil Engineering*, vol. 23, no. 11, pp. 1311–1331, 2019, doi: 10.1080/19648189.2017.1347068.

[55] M. Ferreira and E. Holt, "Addressing ASR in concrete construction in Finland Environmentally-friendly and durable concrete," 2013, [Online]. Available: https://www.researchgate.net/publication/268146928

[56] J. Lahdensivu, P. Kekäläinen, and A. Lahdensivu, "Alkali-silica Reaction in Finnish Concrete Structures," *Nordic Concrete Research*, vol. 59, no. 1, pp. 31–44, Dec. 2018, doi: 10.2478/NCR-2018-0013.

[57] J. W. Pan, Y. T. Feng, J. T. Wang, Q. C. Sun, C. H. Zhang, and D. R. J. Owen, "Modeling of alkali-silica reaction in concrete: A review," *Frontiers of Structural and Civil Engineering*, vol. 6, no. 1, pp. 1–18, 2012, doi: 10.1007/S11709-012-0141-2.

[58] W. Wang and T. Noguchi, “Alkali-silica reaction (ASR) in the alkali-activated cement (AAC) system: A state-of-the-art review,” *Constr Build Mater*, vol. 252, p. 119105, Aug. 2020, doi: 10.1016/J.CONBUILDMAT.2020.119105.

[59] S. Qin, D. Zou, T. Liu, and A. Jivkov, “A chemo-transport-damage model for concrete under external sulfate attack,” *Cem Concr Res*, vol. 132, p. 106048, Jun. 2020, doi: 10.1016/J.CEMCONRES.2020.106048.

[60] G. Prakash, X. X. Yuan, B. Hazra, and D. Mizutani, “Toward a Big Data-Based Approach: A Review on Degradation Models for Prognosis of Critical Infrastructure,” *J Nondestruct Eval Diagn Progn Eng Syst*, vol. 4, no. 2, May 2021, doi: 10.1115/1.4048787.

[61] Q. feng Liu, M. F. Iqbal, J. Yang, X. yang Lu, P. Zhang, and M. Rauf, “Prediction of chloride diffusivity in concrete using artificial neural network: Modelling and performance evaluation,” *Constr Build Mater*, vol. 268, Jan. 2021, doi: 10.1016/j.conbuildmat.2020.121082.

Appendices

Appendix 1. List of mathematical symbols

1) Gradient

For a function f (x , y , z) in three-dimensional Cartesian coordinate variables, the gradient is the vector field:

$$grad(f) = \nabla \mathrm{f} = \left(\frac{\partial}{\partial \mathrm{x}}, \frac{\partial}{dy}, \frac{\partial}{\partial z}\right) f = \frac{\partial \mathrm{f}}{\partial \mathrm{x}} \boldsymbol{i} + \frac{\partial f}{dy} \boldsymbol{j} + \frac{\partial f}{\partial z} \boldsymbol{k}$$

where i, j, k are the standard unit vectors for the x, y, z-axes. More generally, for a function of n variables ψ (x_1 , … , x_n), also called a scalar field, the gradient is the vector field:

$$\nabla \psi = \left(\frac{\partial}{\partial x_1} , \dots , \frac{\partial}{\partial x_n}\right) \psi = \frac{\partial \psi}{\partial x_1} \boldsymbol{e_1} + \dots + \frac{\partial \psi}{\partial x_n} \boldsymbol{e_n}$$

where $\boldsymbol{e_i}$ are orthogonal unit vectors in arbitrary directions.

As the name implies, the gradient is proportional to and points in the direction of the function's most rapid (positive) change. For a vector field $A = (A_1 , \dots , A_n)$, also called a tensor field of order 1, the gradient or total derivative is the $n \times n$ Jacobian matrix:

$$J_A = dA = (\nabla A)^T = \left(\frac{\partial A_i}{\partial x_j}\right)_{ij}$$

- For a tensor field T of any order k, the gradient grad $grad(T) = dT = (\nabla T)^T$ is a tensor field of order k + 1.
- For a tensor field T of order k > 0, the tensor field ∇T of order k + 1 is defined by the recursive relation:

$$(\nabla T) \cdot C = \nabla (T \cdot C)$$

where C is an arbitrary constant vector.

2) Divergence

In Cartesian coordinates, the divergence of a continuously differentiable vector field $F = F_x\boldsymbol{i} + F_y\boldsymbol{j} + F_z\boldsymbol{k}$ is the scalar-valued function:

$$div\ F = \nabla \cdot \mathrm{F} = \left(\frac{\partial}{\partial \mathrm{x}}, \frac{\partial}{dy}, \frac{\partial}{\partial z}\right) \cdot (F_x, F_y, F_z) = \frac{\partial \mathrm{F_x}}{\partial \mathrm{x}} + \frac{\partial F_y}{dy} + \frac{\partial F_z}{\partial z}$$

As the name implies the divergence is a measure of how much vectors are diverging.

The divergence of a tensor field T of non-zero order k is written as $div(\ T\ ) = \nabla \cdot\ T$, a contraction to a tensor field of order $k\ -\ 1$. Specifically, the divergence of a vector is a scalar. The divergence of a higher order tensor field may be found by decomposing the tensor field into a sum of outer products and using the identity,

$$\nabla \cdot (\ A \otimes T\ ) = T(\nabla \cdot A) + (A \cdot \nabla)\ T$$

where $A \cdot \nabla$ is the directional derivative in the direction of A multiplied by its magnitude. Specifically, for the outer product of two vectors,

$$\nabla \cdot (AB^T) = B(\nabla \cdot A) + (A \cdot \nabla)B.$$

For a tensor field T of order $k\ >\ 1$, the tensor field $\nabla \cdot T$ of order $k\ -\ 1$ is defined by the recursive relation

$$(\nabla \cdot T) \cdot C = \nabla \cdot (T \cdot C)$$

where $\boldsymbol{C}$ is an arbitrary constant vector.

3) Pi product notation

A short way to write the product of many numbers is to use the capital Greek letter pi: $\prod$. This notation (or way of writing) is in some ways similar to the Sigma notation of summation.

$$\prod_{i=1}^{n} i = 1 \cdot 2 \cdot 3 \cdot \cdots \cdot n = n!$$

$$\prod_{i=1}^{n} x = x^n (i.e., the\ usual\ n^{th}\ power\ operation)$$

Relation of Pi product to Summation

The product of powers with the same base can be written as an exponential of the sum of the powers' exponents:

$$\prod_{i=1}^{n} a^{c_i} = a^{C_1+C_2+\cdots+c_n} = a^{(\sum_{i=1}^{n} c_i)}$$

4) Nabla symbol (**∇**)

The nabla (∇, aka del) – is a triangular symbol resembling an inverted Greek delta. The name comes, by reason of the symbol's shape, from the Hellenistic Greek word νάβλα for a Phoenician harp and was suggested by the encyclopedist William Robertson Smith to Peter Guthrie Tait in correspondence. The nabla operator ∇ has many important applications in physical problems. In Cartesian coordinates is defined as

$$\nabla = i\nabla_1 + j\nabla_2 + k\nabla_3 = i\frac{\partial}{\partial x} + j\frac{\partial}{\partial y} + k\frac{\partial}{\partial z}$$

There are possible operations with ∇ which are:

1. Gradient

If (f) is a scalar field

$$grad(f) = \nabla f = \left(\frac{\partial f}{\partial x}, \frac{\partial f}{\partial y}, \frac{\partial f}{\partial z}\right)$$

2. Divergence

If (f): is a vector field and $f(x, y, z) = (fx, fy, fz)$,

$$div(f) = \nabla \cdot f = \left(\frac{\partial f_x}{\partial x}, \frac{\partial f_y}{\partial y}, \frac{\partial f_z}{\partial z}\right)$$